UNIVERSITÀ POLITECNICA DELLE MARCHE

ENGINEERING FACULTY

Master of Science in Biomedical Engineering

CLASSIFICATION OF PULMONARY CANCER HISTOTYPES FROM COMPUTED TOMOGRAPHY SCAN

Advisor:

Prof. Laura Burattini

Candidate:

Jafar Hamad

Co-advisors:

Prof. Aldo Franco Dragoni

Dott. Agnese Sbrollini

A.Y. 2020/2021

ACKNOWLEDGMENTS

TO my professor who gave me the chance to be a student at biomedical engineering department as first, moreover accepted me as an intern to learn one of the most interesting aspects "Machine Learning" ……...…….**Prof. LAURA BURATTINI**

To my Co-supervisors who were super helpful and patient, it was a great honor to work with you ……...**DOTT.AGNESE SBROLLINI & DOTT.TOMASSINI SELENE**

To my co-supervisor who was a part of this work……..**Prof. ALDO FRANCO DRAGONI**

To MOM who cannot be described in words and who gave me everything……**WEDAD**

To DAD who always looks at me with pride…..……..**AHMAD**

To my Sisters and brother who make me stronger and unbreakable……

……..**SARA & SAFAA & MOHAMMAD**

To the old companion of this long journey and my best friend in Italy ……...**AYA**

To who was a random college in my hometown but the exile turned him to best friend **AYHAM**

To my buddy and the best Italian man, I am full of trust you will do it as always you encouraged me before each exam ……. **CAPITANO degli SCORPIONI, PESCE, JACOPO**

To the all scorpions, to all our victories ……**Scorpion un joooour ... Scorpion toujoooour**

To my friend who always supports me and gives me a hand…….**RAMA**

To the lovely couple who become my friend from the first meeting ……... **LUNA&PJ**

To the first partner in my first work ever ……**LOUJAIN**

To all my friends in my home country … **LAMA, MAJD, JAFAR, HAIDAR and more** …

To the sweetest and most lovely girl, I have ever known……... **OLA**

THANKS TO EVERYONE I MAY FORGET, YOU ALL IN MY HEART

YOUR SINCERE FRIEND

JAFAR

Abstract

Lung cancer is one of the most deadly and prevalent cancers that affect people, and it was initially designated as a global epidemic in the 1950s when many years of cigarette smoking began to inflict substantial harm. It continues to be the leading cause of cancer-related fatalities in both men and women around the world. With 2.2 million new cases diagnosed and 1.8 million deaths in 2020, lung cancer will be the second cancer type diagnosed and the first cause of cancer death, accounting for 11.4 percent of cancers diagnosed and 18.0 percent of deaths. Since 1987, lung cancer has been responsible for more deaths in women than breast cancer, and it will be the leading cause of death in men, followed by prostate and other cancers.

This led to more interest in doing more research about lung cancer and to understand its symptoms, where the computed tomography played an important role by providing data related to this cancer as images, which seeks more interest in reading and analyzing the images by many researchers, especially last decade that many papers have been published related to segmentation and classification the lung cancer using neural networks and machine learning algorithms.

The aim of this work is to study is to review the most important techniques to segment lung cancer in order to use later for classification. This was done by investigating literature that combined the machine learning segmentation and lung cancer and applying 3DU-net architecture with sets of scans that contain two types of cancer Adenocarcinoma and squamous. This method has been chosen as the most used and effective way to segment the CT scans and provide pure datasets for the next stage which is the classification. those kinds of literature were selected after searching on different search engines such as google scholar, PUBMED, IEEE Xplore, and 12 research were founded related to lung cancer segmentation using neural network 7 of them using U_NET. A paper published by Shaziya et.al in 2018, used U_net architecture in order to segment the lung by inserting the lungs dataset that contains 267 CT pictures of the lungs and the segmentation maps that go with them. 0.9678 and 0.0871, respectively, are their accuracy and loss attained.

Hassani, E L and et.al in 2018, used the U_net model for lung segmentation and before starting using the U_net they applied a manual segmentation that gave the ground truth for the lung parenchyma, they could achieve an accurate segmentation with a Dice-coefficient index of 95.02.

While in Men et al. paper, they proposed 2D-CNN for lung cancer segmentation, Their method consisted of five steps and was based on automatic segmentation with deep active learning, which achieved the best values as the accuracy was 97%, sensitivity 100%, specificity 94%, and AUC 97%.

Q. Hu et al created 2D- Mask R-CNN in combination with K-means for lung segmentation. Their model is based on two stages: Region Proposal Network (RPN), and predicting the class and box offset, and they used both supervised method and unsupervised method that showed better results, its accuracy was 97.68%, sensitivity 96.58%, and specificity 97.11%.

Roth et al. in created a 3D U-net model derivative from 3D-FCN for CT scan segmentation. Their work has been achieved with accuracy reached to 89.4 %.

Zhou et al. proposed Unet++ architecture for lung nodule segmentation based on nested and dense skip connections, their model started with an encoder sub-network. Where The main idea behind UNet++ is to bridge the semantic gap between the feature maps of the encoder and decoder before fusion.

Xiao et al proposed 3D-Res2UNet architecture to segment the lung nodules from CT scans and their method contained 23 layers. This method achieved a good result in the segmentation with where the dice coefficient index reached 95.30% and the recall rate that referred to sensitivity reached 99.1%.

Kaul et al. 2019 proposed a FOCUS-NET neural network with RGB CT scans, and their methods segmented lung cancer with an accuracy of 99.32%, sensitivity 97.57%, and specificity 99.8%, and for skin cancer showed accuracy 92.14%, sensitivity 76.73%, and specificity 98.96%.

In 2021, Tan et al. proposed the LGAN model to segment the lung from CT scans based on the Generative Adversarial Network structure, where the neural network is trained to generate the lung mask based on the grayscale.

Xu et al proposed a 2D -CNN neural network to segment lung parenchyma from CT scans. They split CT scans into image patches, then performed a clustering algorithm with two categories twice, that segment the lung parenchyma with accuracy up to 99.2%, Sensitivity = 98.8%, Specificity= 99.5%, and AUC = 99.91%.

In the other hand, for classification lung cancer from CT scan techniques, and review has made by searching in 3 search engines google scholar, IEE explorer and PUBMED, that's led us to find 8 research, 5 of them used CNN neural network.

In 2018 Zotin A et al. proposed LSTM neural network to classify lung cancer combining it with CNN neural network which extracted the features from the 2D images in order to extract the map features from the previous layer. The accuracy of this method was 97% in classification between normal and cancer cases.

Maolood IY et.al, proposed Distance LSTM with two different datasets as a neural network, where three gates distinguish the LSTM architecture "forget gate, input gate, and output gate", their method showed 78.96 and 82.55 for accuracy and area under the curve AUC in the first dataset, 86.97 and 86.97 for accuracy and area under the curve AUC in the second dataset.

Cai et al. in 2014 proposed a feed-forward CNN neural network to classify lung image patches with interstitial lung disease (ILD), the authors built their network with 5 different layers showing the accuracy of more than 90% in the classification of interstitial lung disease (ILD).

Lakshmanaprabu et al 2019, proposed ODNN, their architecture input was features extracted by the histogram, texture, and wavelet of the image. The accuracy method raised to 94.56% and the sensitivity and specificity were 96.2% and 94.2% in the classification of lung cancer.

Alakwaa et al in 2019 proposed two architectures to classify lung cancer "U-net and 3D-CNN", they used thresholding for initial segmentation to segment the lung from CT scans and feed them into 3D-CNN for classification, this approach provided a classification accuracy of Lung Cancer with 86.6% and AUC with 83%.

(Olulana et al) 2020 proposed a hybrid algorithm for nodule generation of Lung from CT scans composed from CNN with 3D Convolutional LSTM algorithm, where the CNN used for features extraction. The authors produced a 3D tensor that flows through each cell by convolving the input and the previous hidden states, their method achieved 97.2% as accuracy for detection of the progression of lung cancer.

In (Polat and Mehr) 2019 proposed a hybrid technique composed from 3D-CNN with SVM for detection of lung cancer nodules from CT scan, the features have been extracted manually to fed their backpropagation CNN algorithm, this method provided 91.81% for accuracy, 88.53 and 94.23 for sensitivity and specificity, respectively, for detection cancer.

In 2020 Sibille et al provided 2D- CNN to classify two datasets one was with Lung Cancer and the second was with lymphoma, where they used for segmentation two experts to do it by using a volume-of-interest tool to classify the lesion into suspicious for cancer or nonsuspicious for cancer, then they used threshold for automatic segmentation, after that thy imported the data to the CNN architecture to classify and localize the disease in both datasets, their methods achieved with the first dataset 88.4% as an accuracy .75.4% sensitivity, 95.8% specificity and 95% as AUC, and for the second dataset the results were (Accuracy: 88.6%, Sensitivity 87.1%, Specificity 99.0%, and AUC 98%)

The methods above are used for either segmentation and classification for the lung cancer images provided from CT scans where CNN was the most used for classification, besides it was used for segmentation in some papers, where both of Men et al. paper where their results 97% sensitivity 100% specificity 94% AUC 97%, Q. Hu et al in showed accuracy 97.68%, sensitivity 96.58%, and specificity 97.11%, while Xu et al in using CNN technique for lung segmentation and their methods, while either of Shaziya et.al in 2018 and Hassani, E L and et.al in 2018, Roth et al. in 2018, Zhou et al. in 2018, and Xiao et al in 2020 used U_net

Those methods applied for segmentation and classification in different ways, where LSTM and CNN were the most used techniques for image classification and sometimes researchers used a combination of both to show more efficiency especially since CNN is powerful in feature extraction with no need for pre-processing on some cases, providing more efficient results and for segmentation, it was noticeable that U_net was the most common approach used by researchers due to the feature extraction using the downsampling and upsampling processing.

Machine learning and its uses in medical imaging analysis or segmentation have many approaches to follow and the experiments done by the papers above showed that the combination of two types of architecture is a better solution, providing more accurate results, making it more commonly used in the past few years.

Contents

List of Figures

List of tables

Chapter I

The respiratory system

1. Chapter 1: The respiratory system

1.1 Anatomy and Structure

Respiration is the act of breathing, to be specific inhaling (inspiration) oxygen "O_2" from the environment into the lungs and exhaling (expiration) into the environment carbon dioxide "CO_2". The organs that made up the respiratory system which involved in breathing are the nose, pharynx, larynx, trachea, bronchi, and lungs, as shown in Fig. 1.1.

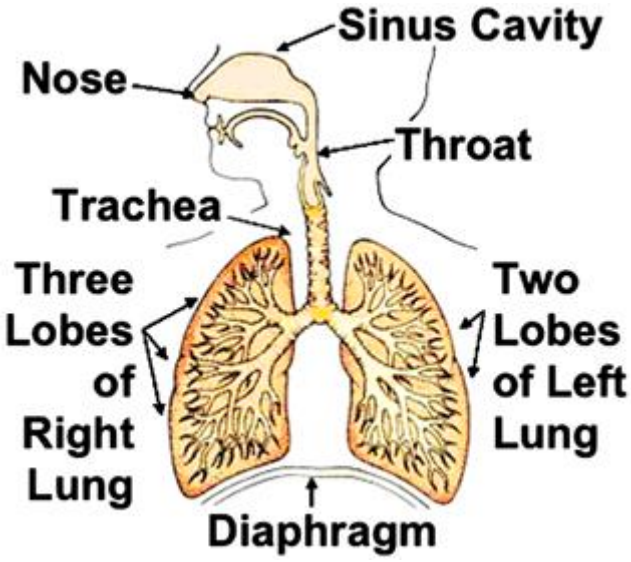

Fig. 1.1 Schematic representation of the respiratory system and its main components [1].

Those organs belong to the two respiratory system parts, where the upper airways part and the lower airways part. The nose, with its nasal cavity, frontal sinuses, maxillary sinus, larynx, and trachea composes the upper respiratory tract while the lower respiratory tract includes the lungs, bronchi, and alveoli [1].

1.1.1 The Nose

The nose is a semirigid texture made of bone and cartilage, contained three regions within the space behind the nose that is called the nasal cavity which is separated into right and left halves. Those regions contained within each nasal cavity are the vestibular, olfactory, and respiratory regions.

The vestibular region works as a defense line by trapping large particles in the incoming air using its hairs which are called vibrissae, to protect the airways and lungs.

While the respiratory region works on heating the incoming air temperature, so the airways and lungs do not dry out. [2][3]

1.1.2 The sinuses

Sinuses surround the nasal cavity lighten the skull, help warm and moisten the air inhaled and act as resonance chambers for speech, naming of sinuses parts coming from facial pones where they are located: the ethmoid, sphenoid, maxilla, and frontal bones as shown in figure (1.2) below [4].

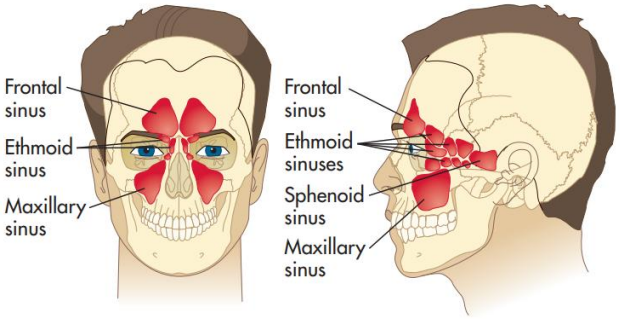

Figure 1.2 The sinuses [4].

1.1.3 Pharynx

The incoming air passes after entering from the mouth or nose directly to the Pharynx which is a hollow and muscular chamber that lies above the Larynx. It is divided into 3 segments: Nasopharynx, Oropharynx, and Laryngopharynx. Pharynx also plays a role in making sound and production of speech.

1.1.4 Larynx

Known also as the voice box, which is very important for the speech. It is a triangular chamber located in the neck, where the vocal cord is controlled by several types of cartilage that composed the larynx, such as the thyroid cartilage and the cricoid cartilage that playing an important role in controlling the airway providing structures and support, so they do not collapse and block the flow of air into and out of the lungs. Another cartilage called the epiglottis covers the larynx during swallowing. The vocal cords are the area of division between the upper and lower airways [3].

1.1.5 Trachea and Bronchi

The lower part of the respiratory system starts with the trachea, as an extension from the cricoid cartilage of the larynx to the fifth thoracic vertebrae, playing the main passage role to the lungs. Since the upper part of the trachea is connected to the larynx, it is covered by the epiglottis, which is a small flap of tissue called the, prevents food and liquids from entering the trachea.

Rings of cartilage distinguish the trachea, and they are important to keep the airway open, those rings have a C shape, not a closed circle, to allow for the expansion of the esophagus during food swallow.

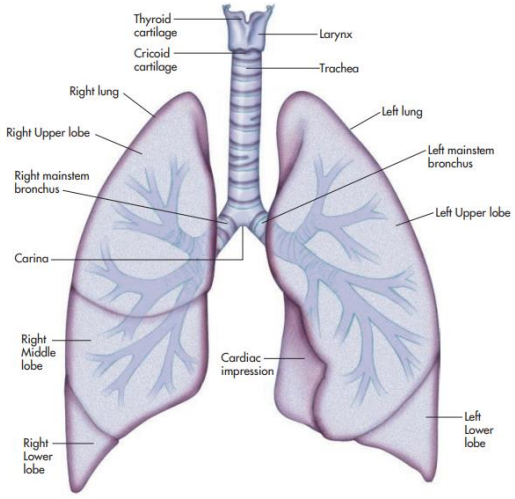

Figure 1.3 The tracheobronchial tree [3]

The trachea is the largest bronchus, and it splits in the centre of the chest as the first branching "right and left bronchi" and the site of splitting carina. The left primary bronchus splits into two secondary bronchi, while the right primary bronchus splits into three secondary bronchi, based on the number of lobs in each lung. That bronchus splits more and more inside the lung into tubes with smaller and smaller diameters which called bronchioles, and the terminal bronchioles come after with 0.5-mm diameter which marks the area directly before the gas changing or respiratory zone in the lung, that contains the respiratory bronchiole where the gas exchange occurs here but in a very small amount. Finally, this airway ends with the Alveolar ducts and their Alveolus, which is the zone of gas exchange, the walls of the alveolar ducts are completely made up of simple squamous cells.

1.2 The Lung Anatomy

Lungs are one of the most important vital organs in the human body, as a major part of the respiratory system, where the primary function of this system is exchange. O_2 (which is needed for cells to function) from the external environment is transferred into our bloodstream while CO_2 (a waste product of cellular function) is expelled into the outside air.[1] This organ is a paired cone-shaped lying in the thoracic cavity where the heart separates from each other and is bordered inferiorly by the diaphragm.

where the lungs are separated from each other by the mediastinum, an area that contains the following: heart and its large vessels, trachea, esophagus, thymus, and lymph nodes.

Because the size of the lung is dependent on its volume. The normal weight range of each lung in an adult is roughly 300 to 450 g, the right lung is slightly larger than the left by a volume ratio of 53% to 47, [5] and because of their stretchable nature, the lungs contract to about one-third their size when the thoracic cavity is opened. [6] wherein adults, the total amount of air after deep breathing is approximately 5L contained in the lung.

Fibrous major fissures separate the upper from lower lobes of both the right and left lungs and an additional minor fissure partitions the right middle lobe. These fissures may be anatomically complete or incomplete. This is potentially important as air can move from one segment or lobe to another via collateral ventilation if fissures are incomplete.[7]

According to Jackson and Huber in 1943 who proposed a system that segmented the lungs into bronchopulmonary segments, where The right lung has 10 segments and the left lung has 8, their system was acceptable to Thoracic surgeons, bronchoscopists, radiologists, and anaesthetists [8].

Table (1.1) The bronchopulmonary segments

Right Lung (10 Segments)	left Lung (8 Segments)
Right upper lobe bronchus (3 segments) • Apical • Posterior • Anterior	Left upper lobe bronchus (4 segments) • Apical posterior • Anterior • Superior lingula • Inferior lingula
Middle lobe bronchus (2 segments) • Lateral • Medial	

Right lower bronchus (5 segments)	Left lower lobe bronchus (4 segments)
• Superior • Medial basal • Anterior basal • Lateral basal • Posterior basal	• Superior • Anteromedial basal • Lateral basal • Posterior basal

Each bronchopulmonary segment is pyramidal in shape with its apex pointing toward the center of the lung and its base toward the pleural surface. It is surrounded by connective tissue septas, which are continuous with the pleural surface and prevent air collateralization between segments somewhat [8]

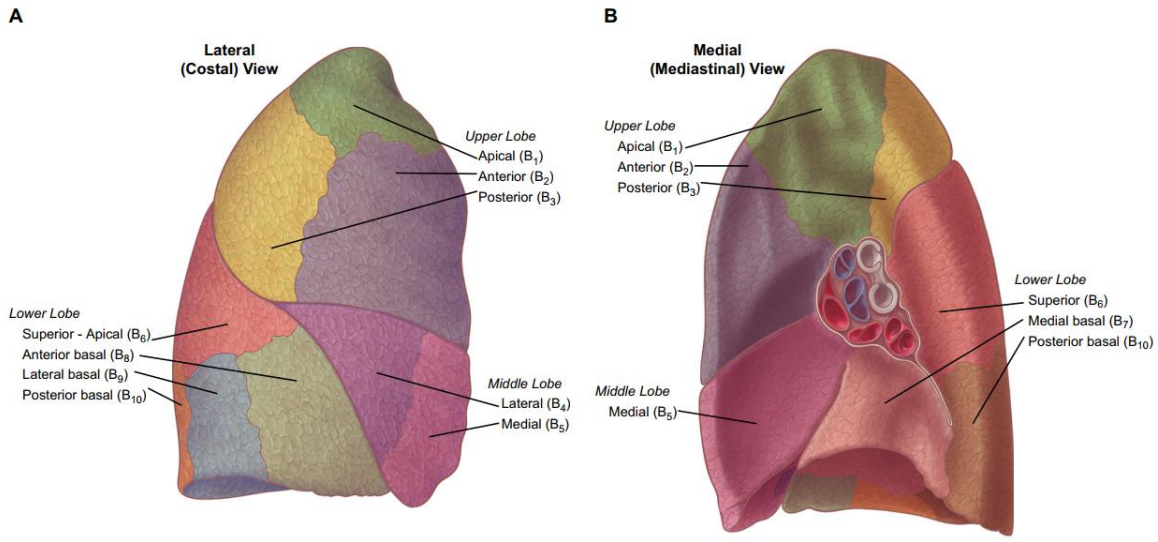

Figure 1.4 The right bronchopulmonary segments [8].

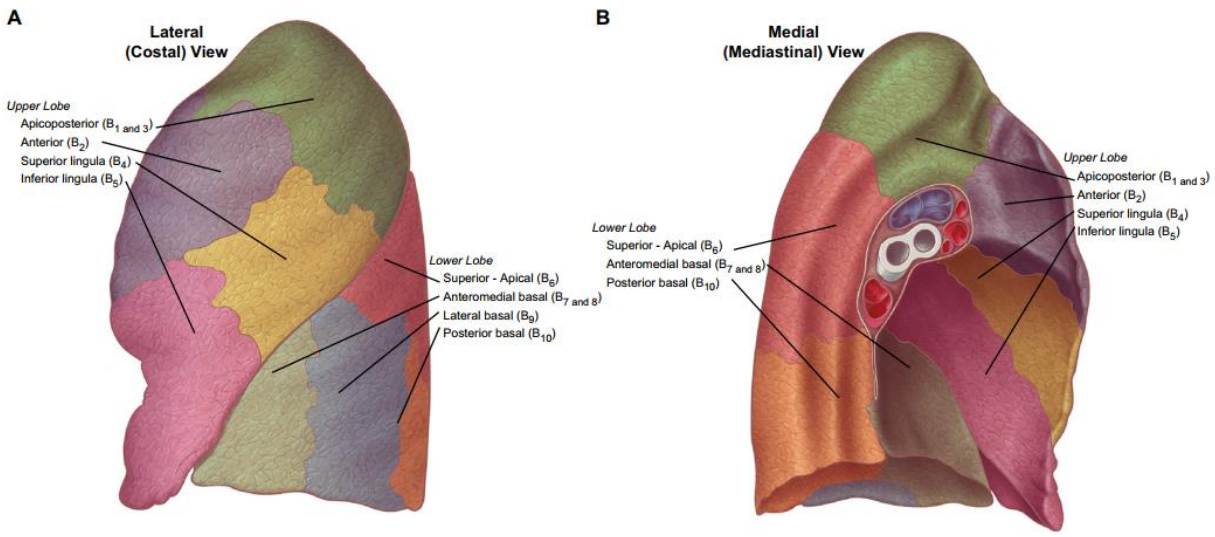

Figure 1.5 The left bronchopulmonary segments [8].

1.3 Lung Surface

After the air passing through the trachea, the next enters is the bronchial tree, a series of branching tubes of progressively smaller diameter that lead to the lung surface where the gas exchange only occurs at the lung surface. For this reason, the volume of air residing within all of these finely branched airways. Reaching the alveolar ducts and its air sacs "alveoli" as shown in the previous paragraph.

Where the wide surface of the alveolar is equivalent to 70 square meters (about the size of a tennis court), allowing efficient gas exchange, O_2, and CO_2, between the blood and the air of the external environment. Two types of alveolar epithelial cells: type I is a single layer of flattened squamous epithelial cells that have a base membrane and compose the wall of the alveoli, the second one is type II alveolar epithelial cells, that also participate in the gas exchange in addition of secreting the fluid containing surfactants that play role in reducing the surface tension and prevent the collapse of the alveoli.

The terminal air sacs are surrounded by numerous pulmonary capillaries, tiny blood vessels, which consist of endothelial cells and their basement membrane as shown in figure (1.6), all together make up the respiratory membrane [9].

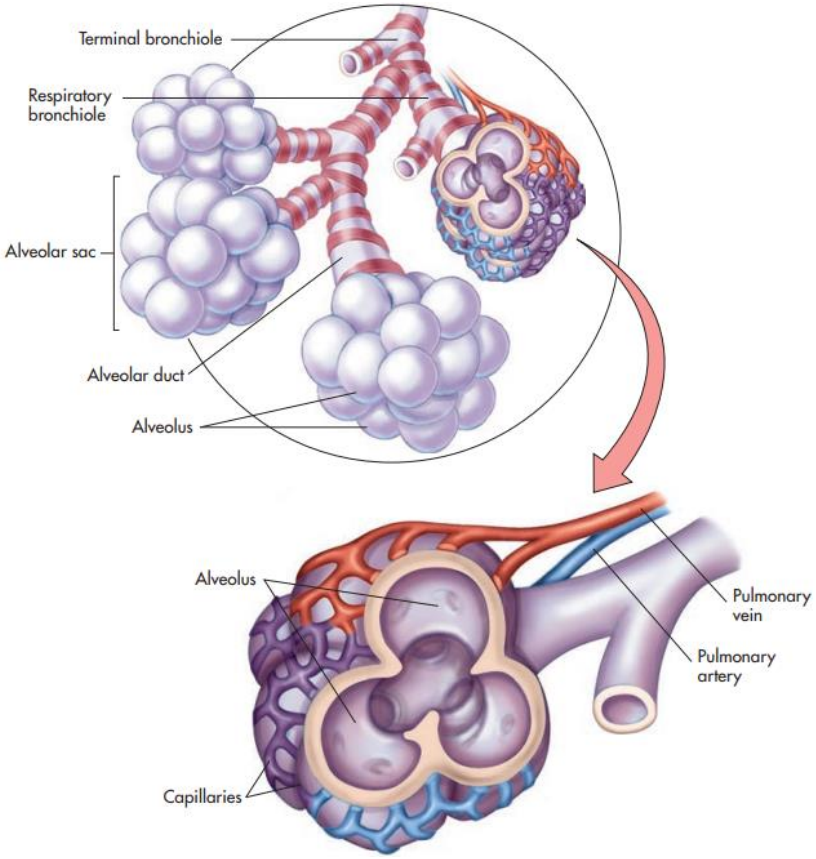

Figure 1.6 Conduction and gas exchange structures [9].

1.4 Physiology of Respiration System

Lungs play the most important role in breathing which following a mechanism that controls this action, The bulk flow exchange of air between the atmosphere and the alveoli is referred to as ventilation or breathing. Depending on whether air enters or exits the body, it is possible to recognize a different phase of ventilation: inspiration (inhalation), which is the movement of air from the external environment through the airways into the alveoli during breathing, and expiration (exhalation), which is the movement in the opposite direction. A single respiratory cycle consists of an inspiration followed by an expiration. During the entire respiratory cycle, the right ventricle of the heart pumps blood through the pulmonary arteries and arterioles and into the capillaries surrounding each alveolus. In a healthy adult at rest, approximately 4 litters of fresh air enter and leaves the alveoli per minute, Ventilation describes the flow Q of air into the lungs. In the two verses, this flow is driven by a pressure gradient ΔP between two points and limited by the fluid dynamic resistance R . When the fluid is forced to move within conduct, these physical quantities are tied by Poiseuille's law [9]:

$$Q=\Delta P/R \qquad (1)$$

it is clear that ventilation happens to be the mechanism that the body has to modulate the pressure gradient, achieving the task of taking in oxygen and bringing out carbon dioxide. Indeed, the body has also mechanisms to modulate the fluid dynamic resistance. Being the length of both the respiratory tract and air viscosity constant in normal conditions, the fluid dynamic resistance can change with the section of the bronchioles, since the section of trachea and bronchi is fixed by a series of cartilaginous disks. Bronchioles are collapsible tubes and a decrease in their diameter can suddenly turn them into a significant source of airway resistance. This mechanism is called bronchoconstriction and aims to avoid discomfort situations as the inspiration of cold air. The converse process, bronchodilation, intervenes with expired higher CO2 levels. For air to move into the alveoli, the pressure inside the lungs must become lower than atmospheric pressure. According to Boyle's law, an increase in volume will create a decrease in pressure, hence inspiration aims to enlarge the volume inside the thoracic cage by the contraction of certain skeletal muscles and diaphragm.

1.4.1 Gas exchange:

The aim of ventilation is to bring inside alveoli a flow of air. Then, the process follows with external respiration or gas exchange, which aims to regulate three fundamental physiological variables:

1. Oxygen level. Arterial oxygen delivery to the cells must be adequate to support aerobic respiration and ATP production.
2. Carbon dioxide level. Waste product during Krebs's cycle, excretion of CO2 from the lungs is important for two reasons: high levels of CO2 are a central nervous system depressant, and elevated CO2 causes a state of acidosis (low pH).
3. Plasma pH. Maintaining pH homeostasis is critical to prevent the denaturation of proteins. The respiratory system monitors plasma pH and uses changes in ventilation to alter it.

Individual gases such as oxygen and CO2 diffuse from alveolar air space into the blood. From what concerns gases, they move from regions of higher partial pressure (i.e. the contribution of a single gas to the total pressure of gas mixture) to the region of the lower one. In normal conditions, alveolar PO2 at sea level is about 100 mmHg. The PO2 of "deoxygenated" pulmonary capillaries arriving at lungs is about 40 mmHg, hence oxygen moves to capillaries from alveoli. Since the blood in the vessel is under a gradient of pressure, this situation of exchange will never reach equilibrium, and the oxygen pathway is only in this direction. When

the arterial blood reaches the systemic capillaries, the gradient is reversed: cells are continuously using oxygen in oxidative phosphorylation, which is transformed in CO2 and water. Therefore, the intracellular PO2 is 40 mmHg, against the 100 mmHg of arterial blood. Here oxygen flows from capillaries to cells. Conversely, PCO2 is higher in tissues than in systemic capillary blood because of CO2 production during cellular metabolism. Cellular PCO2 in a person at rest is about 46 mmHg, compared to an arterial plasma PCO2 of 40 mmHg. This gradient causes CO2 to diffuse out of cells into the capillaries, and systemic venous blood averages a PCO2 of 46 mmHg. At the pulmonary capillaries, the process reverses. Venous blood bringing waste CO2 from the cells has a PCO2 of 46 mmHg, against the alveolar PCO2 of 40 mmHg. Thus, CO2 drains from capillaries and moves into the alveoli [9].

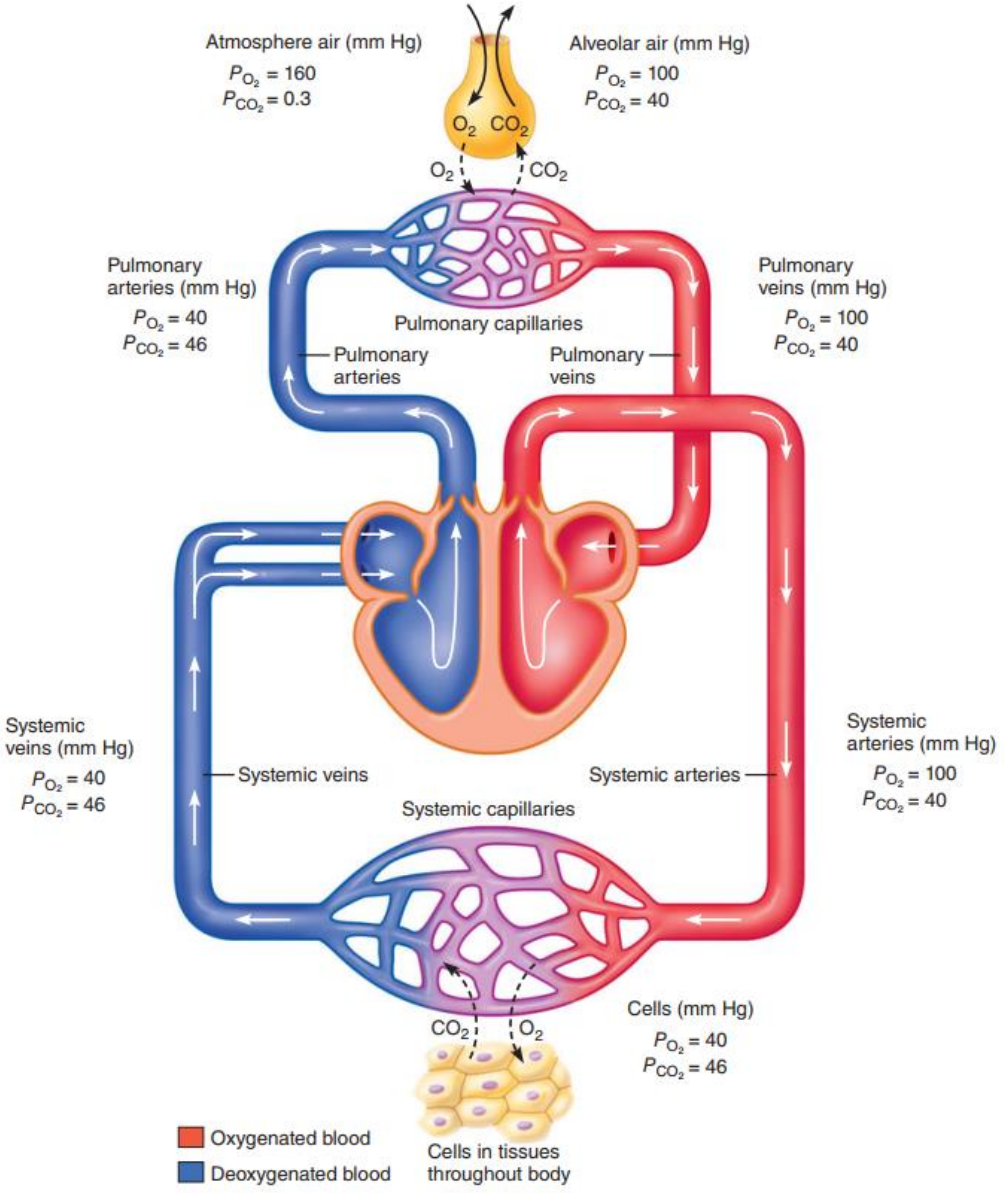

Figure 1.7 Gas Exchange and Regulation of Breathing [9].

Chapter II

The Lung Cancer

2. Chapter 2: The Lung Cancer

2.1 Overview of lung cancer

Lung cancer is considered as one of the most mortality and common cancer that affect humans, and historically lung cancer was first given status as a global epidemic in the 1950s when many years of cigarette smoking started to cause significant damage. It keeps on being the main source of cancer-related deaths among males and females around the world. where 2.2 million new cases diagnosis and 1.8 million deaths, this classified it as the second cancer type diagnosed and the first reason for cancer death in 2020, approximately it is representing (11.4%) cancers diagnosed and (18.0%) deaths, and since 1987, lung cancer is responsible for more deaths in women than breast cancer, and taking the lead of death causes in male followed by prostate and colorectal cancer [10], as the main causes of lung cancer are smoking with 90 % of the cases attribution to the smoking.

The uncontrolled cell growth in the lung tissues is what characterized this disease, where the two major types of cancer are small–cell lung carcinoma (SCLC) and non-small-cell lung carcinoma (NSCLC), while the highest percent for the patient infection is about 80% to 85% for the (NSCLC) comparing to 10 % to 15 % approximately for (SCLC) [11].

2.2 Pathogenesis and symptoms

Lung cancer has the same way of developing many cancer types, it starts by inactivation the genes tumor suppressor oncogenes activation [12], and mutations caused by carcinogens in these genes that led to the development of cancer, such as K-ras proto-oncogene mutations that cause 10-30% of lung adenocarcinomas, fusion an EML4-ALK tyrosine kinase gene is responsible for 4% of non-small cell lung carcinomas, also the inactivation of genes tumor caused by histone tail modification, micro RNA regulation-may or epigenetic changes-such as alteration of DNA methylation, all together are factors of cancer developing.

Mutations and amplification of EGFR (Epidermal growth factor receptor) are common in non-small-cell lung carcinoma because this gene is responsible for regulates cell proliferation, angiogenesis, apoptosis, and tumor invasion [13].

On the other hand, squamous-cell lung carcinoma is caused by abnormal activation of stem cells in proximal airways, and the stem cells that express keratin 5 are more likely to be affected [14].

As result, lung cancer has several symptoms and signs on the human body such as cough where central airway cancer-causing post obstructive pneumonia or lymph node enlargement, and Dyspnea considered as an early indication of tumor in the main airway; and sometimes associated with unilateral wheeze. Also, Hemoptysis Blood-streaked sputum, usually accompanied by abnormal chest x-ray but it is rarely severe; Chest pain Nonspecific, aching pleuritic pain is a sign of its spread to the pleural surface [15].

2.3 Histopathology

The broad divisions of SCLC and NSCLC represent more than 95% of all lung cancers.

2.3.1 Small Cell Lung Cancer SCLC

It comprises 10 % to 15 % approximately of all lung cancers, and each year in the United States there are more than 30,000 new cases. This kind of lung cancer is usually located in a peribronchial with infiltration to the peribronchial tissue and bronchial submucosa. Usually, the bronchial obstruction is occurred by circumferential compression, although endobronchial lesions can happen rarely. The tumor is white-tan, friable and soft, and frequently shows wide necrosis. With advanced disease, the bronchial lumen may be obstructed by extrinsic compression. SCLC may present as a solitary coin lesion in up to 5% of cases.

In 2004 WHO classifications there are 2 types of SCLC: SCLC (with pure SCLC histology) and combined SCLC (with a mixture of any non–small cell type) [16].

The SCLC cells are small and have a circulate to fusiform appearance, tiny cytoplasm, finely granular nuclear chromatin, and the nucleoli are missing or inconspicuous. Nuclear smearing and molding of nuclear chromatin as an effect of crush artifact may be conspicuous. It is usually extended, necrosis and mitotic rates are high, with an average of 80 mitoses per 2 mm^2. The growth pattern usually consists of diffuse sheets, but rosettes, peripheral palisading, organoid nesting, streams, ribbons, and rarely, tubules or ductules may be present. The basophilic encrustation of vessel walls, also known as the Azzopardi effect, is often seen in necrotic areas. the reliable diagnosis of SCLC is in small biopsies and cytology specimens [17].

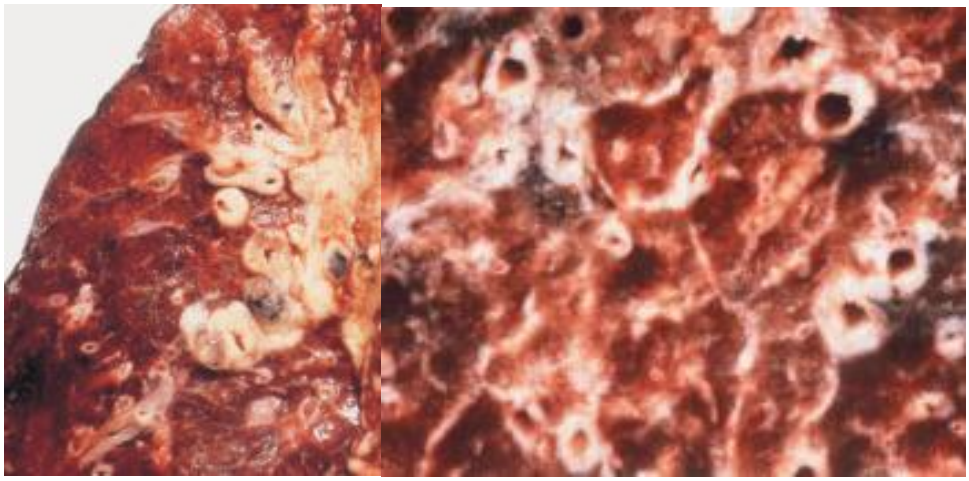

Fig 2.1 The Small cell carcinoma [17].

Combined SCLC that shown in figure (2.2) below is a combination of SCLC and non-small cell carcinoma usually the adenocarcinoma, squamous cell carcinoma, or large cell carcinoma but less commonly spindle cell or giant cell carcinoma, where 4% to 6% of cases are a combination of SCLC and large cell carcinoma, and 1% to 3% of SCLC may be combined with adenocarcinoma or squamous cell carcinoma [17].

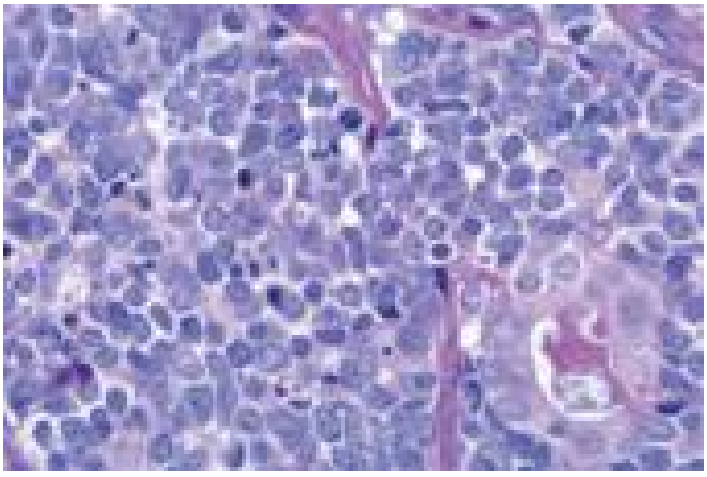

Fig 2.2 The Combined SCLC [17]

2.3.2 Non-Small Cell Lung Cancer

And there are five types:

1- Squamous cell carcinoma:

Is one of the most popular lung cancer types in the USA with approximately 20% among them, and it is characterized by the presence of intercellular bridges squamous pearl formation, and individual cell keratinization. two-thirds of squamous cell carcinomas are located and known as central lung tumors, where the remaining third are located in the peripheral.

This kind grows often in segmental bronchi and involvement of lobar and mainstem bronchus occurs by extension. Different kinds can appear as Squamous cell carcinomas such as papillary, clear cell, small cell, and basaloid subtypes, and often arise a pattern of exophytic endobronchial growth as shown in figure (2.3) below [18].

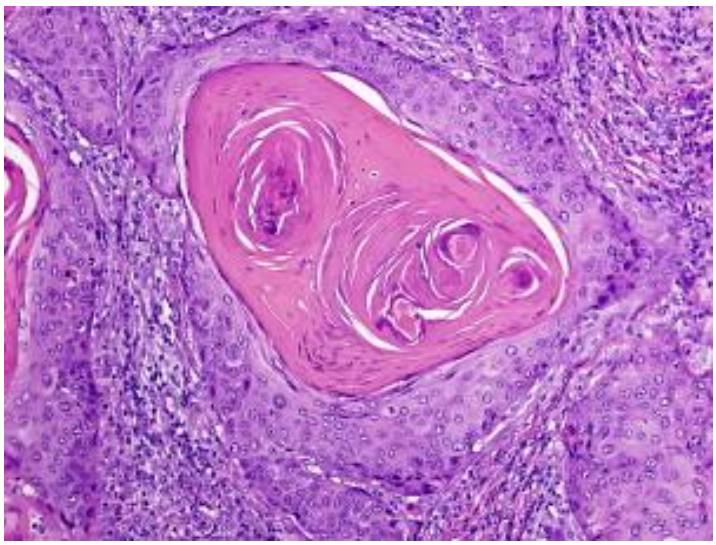

Fig 2.3 Squamous cell carcinoma [18]

2- Adenocarcinoma

It's a malignant epithelial tumor that can be noticed with glandular differentiation or mucin production, papillary, bronchioloalveolar, or solid with either mucin growth patterns or a mixture of these patterns. It represents the most common cancer type in many countries "38% of all lung cancers in the United States". Most cases are shown in smokers but it develops more than any other type of lung cancer in individuals who have never smoked (especially women) [18].

Adenocarcinomas have peripheral nodules smaller than 4.0 cm in size, rarely shown in a central location as a hilar or perihilar mass. 15% of cases have been seen in pleura and chest wall involvement, and hilar adenopathy has less frequently compared with other forms of lung cancer, anyway, what distinguishes the adenocarcinoma from the other histologic subtypes of lung cancer are the patterns that adenocarcinoma shows in such as solid nodules (solid-density), ground-glass opacities (non-solid, air-containing) and mixed solid/ground glass (part solid, subsolid) opacities, and when more solid component compared to ground glass component, the greater the likelihood of invasive growth as seen in figure (2.4) [19]. Adenocarcinoma cells may be single or arranged in three-dimensional morulae, pseudo-papillae, true papillae with fibrovascular cores and/or sheets of cells. and its borders are typically sharply delineated. The

Cytoplasm can appear in different volumes, typically cyanophilic and more translucent, distinctly homogeneous or granular, and in others are foamy due to abundant small indistinct vacuoles. A single large mucin-filled vacuole may be prominent and, in some cases, distends the cytoplasm and compresses the nucleus to one margin, and form a signet-ring cell [17].

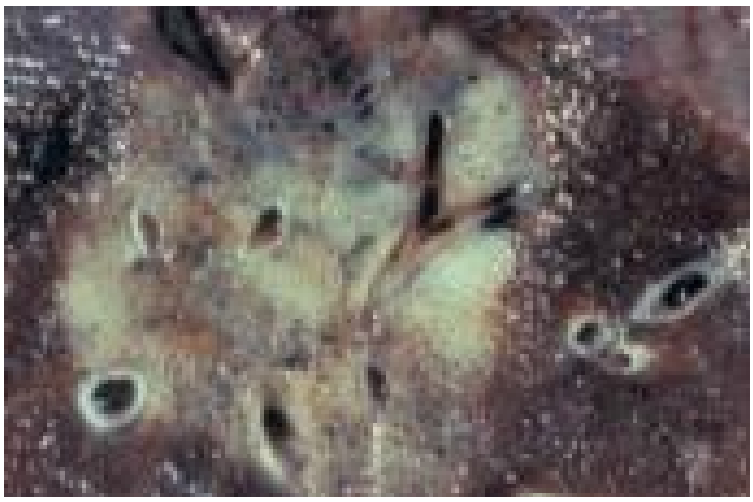

Fig 2.4 Adenocarcinoma with bronchioloalveolar pattern [19]

3- Adenosquamous carcinoma

It represents 0.6% to 2.3% of all lung cancers and contains cells from both adenocarcinoma and squamous carcinoma with 10% of each at least according to WHO [20] where the two components may be separate or may merge and mingle. one could be more than other or maybe seen in equal proportion. The degree of differentiation of each component is not interdependent and is variable. This kind is recognized by central scarring and puckering of the overlying pleura or indentation, additionally, some could show a rim of ground-glass opacity, they are located usually in the periphery of the lung, showing the same features as other non-small cell carcinomas, this features that distinguish adenosquamous carcinoma are the same for squamous carcinoma and adenocarcinoma, and by electron microscopy, features of both cell types are common but tumor classification is based on light microscopy [17].

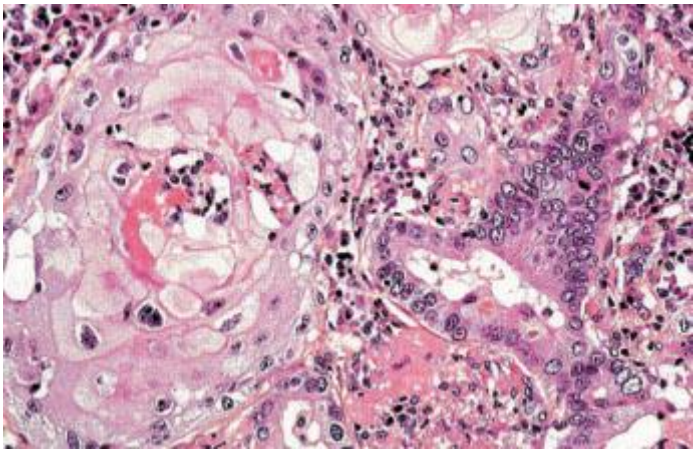

Fig 2.3 Adenosquamous carcinoma [17]

This figure is for adenosquamous carcinoma showing a squamous cell lobule on the left, adjacent to an acinar adenocarcinoma on the right.

4- *Large cell carcinoma*

it comprised 3% of all lung carcinomas, these tumors are mostly represented in the lung periphery, although they may be located in the center as large necrotic tumors, that develops in the outer regions of the lungs and tends to grow rapidly and spread more aggressively than some other forms of lung cancer [21]. Large cell carcinoma is a diagnosis after exclusion of squamous cell or glandular differentiation by light microscopy. the tumors are usually composed of sheets and nests of large cells that have prominent nucleoli and vesicular nuclei [17], shortness of breath and fatigue are its symptoms but chronic cough and coughing up blood are considered as later symptoms [21].

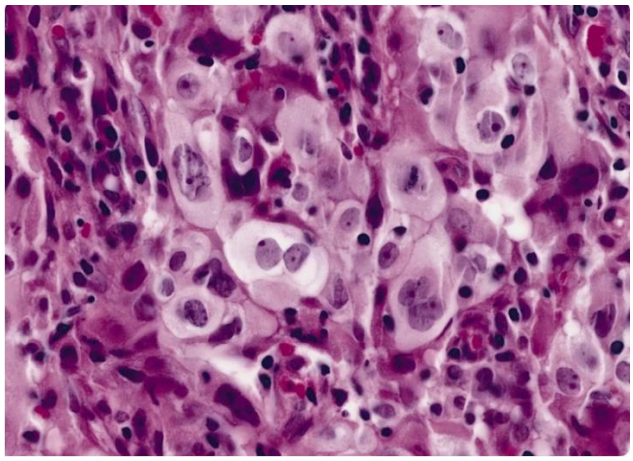

Fig 2.4 Large cell carcinoma [21]

5- *Carcinoid tumors*

Representing 1% to 2% of all lung tumors, where about 50% of patients show no symptoms at presentation. Usually, most of the patients are between 45 to 55 years but it is also considered the most common lung tumor in childhood. It is located in the center with a frequent polypoid endobronchial component, while the peripheral ones are found in the subpleural parenchyma. It is recognized by having moderate eosinophilic, finely granular cytoplasm with nuclei possessing a finely granular chromatin pattern and the nucleoli are inconspicuous in most carcinoid tumors. The forms of this cancer can be in different patterns like spindle cell, palisading, trabecular, rosette-like, papillary, sclerosing papillary, glandular, and follicular patterns. Whilst its symptoms are hemoptysis, post obstructive pneumonitis, and dyspnea [22].

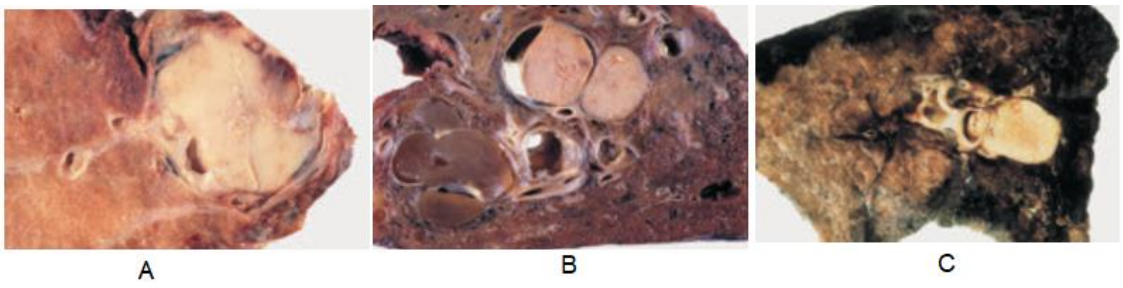

Fig 2.5 Carcinoid tumors [22]

Figure (2.5) above, shown: A Central bronchial carcinoid tumor in a 26-year-old woman. B More peripherally located carcinoid tumor with bronchiectasis. C Typical carcinoid presenting as round, partially endobronchial mass.

2.4 Diagnosis Modalities

Regularly, the diagnosis of NSCLC presents in the advanced stage of the disease. 50% to 75% of patients suffering from cough as the most common symptom, then hemoptysis, chest pain, and dyspnea but laboratory abnormalities or paraneoplastic syndromes are considered as less common symptoms [23]. The diagnosis requires determination of the spread of the tumor to characterize the TNM (Tumor, Node, Metastasis) stage, which will define the way how treats cancer. Where there are two ways to diagnose (invasive test or imaging test)

A study by Danish researchers made a comparison of the staging with (PET) positron emission tomography and CT versus the traditional invasive way (mediastinoscopy and mediastinal lymph node biopsy with echoendoscope) and they found, there was a better classification of N stage diagnosis with PET/CT. Any positive node on PET-CT must be sampled [24][25]. for this reason, and when an individual reports symptoms that could lead to lung cancer, the chest radiograph is one of the first investigative steps, which may show a mass, for example,

consolidation (pneumonia), atelectasis (collapse), widening of the mediastinum (suggestive of spread to lymph nodes there) or pleural effusion [11]. CT imaging is typically used to provide more information about the type and extent of the disease. Bronchoscopy or CT-guided biopsy is often used to sample the tumor for histopathology. For that, medical image reports must reflect the TNM (Tumour, Node, Metastasis) classifications:

2.4.1 Invasive Test

This way is used when the patient showed the symptoms of cancer, Usually, it confirms the presence of a tumor by taking a sample in 3 different ways, and the actual diagnosis is made by looking at lung cells in the lab.

The cells can be taken from lung secretions (mucus coughed up from the lungs), (thoracentesis) fluid taken from the area nearly the lung, or (biopsy) from a doubtful area using a needle or surgery.

2.4.1.1 Sputum cytology

It is a non-invasive technique, where a sample of sputum took from mucus coughed up from the lungs to be examined in the lab to figure out if it has cancer cells, those samples collected either spontaneously or induced in patients who are unable to provide a sample and the ideal sample is from a deep spontaneous cough. Five samples will be collected from the patient on consecutive days which are separately examined, the reasons for obtaining multiple samples are due to the heterogeneity of the sputum smear, and finding relatively few diagnostic cells in each sample [26].

2.4.1.2 Thoracentesis

Used with the pleural effusion, when the fluid has collected around the lungs, some of it can be removed to be diagnosed to see if it is caused by cancer, that 15% of lung cancer patients suffer from pleural effusion, but this symptom could be a reason for another disease such as heart failure or infection [27].

Thoracentesis is an invasive technology, where the skin will be numbed and by using a hollow needle that is inserted between the rib cage to remove the fluid, some of the fluid will be taken to the lab to searching for cancer cells [28]. other tests could be useful to ensure if the sample is a malignant (cancerous) pleural effusion or not.

2.4.1.3 Needle biopsy

Using a hollow needle to get a sample of the indeterminate pulmonary nodule, where the pulmonary nodule can be reached very easily by the needle biopsy, this method is considered

less invasive because it doesn't require a surgical incision. Computerized tomography can be used in this technique as very small lung nodules can be detected in a computerized tomography scan with high efficiency [28].

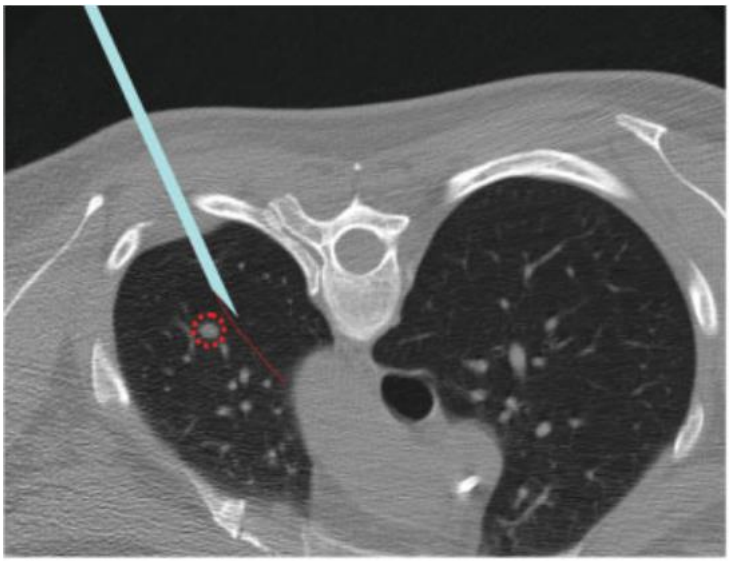

Fig 2.6 needle biopsy guided by CT scan [28].

2.4.2 Imaging Test

Imaging tests are completely non-invasive techniques, providing images of the lung and cancer with a difference in quality based on the methods used. Those methods are the X-ray chest radiography, (CT), magnetic resonance (MR), and positron emission tomography (PET) used for detection, characterization, staging, and follow-up of the growth of lung cancer. Today (PET/CT) is considered the best technique for imaging lung cancer because provides details and information about the localization and extent of tumor expansion, that is, it provides anatomical information about cancer, while positron emission tomography provides metabolic information, so the combination of these two techniques is the best way to collect cancer information [29].

2.4.2.1 X-Ray

It is used for chest radiography and considered the most common technique for the lung imaging test and diagnosis of many pulmonary diseases around the world because of its simplicity, cheapness in use, lower radiation compared to others, its provision of good information and many other advantages [30], its ability to develop through years helped also to contribute increasing in its use especially after conversion from film-based to digital radiographic (DR) systems that provide better, more quality images and reduce the radiation dose [31] the image processing techniques that use with digital radiography are temporal

subtraction and dual-energy subtraction to increase the accuracy of diagnosis, by taking two images at two different times for the chest in posterior-anterior positions and subtraction of each other will provides the temporal subtraction [30]. While the dual-energy subtraction is based on the differentiation between calcified and non-calcified structures in absorbing the radiation as a function of exposure voltage [32].

2.4.2.2 CT

It is the second most important imaging technique of the chest. In 1991 the CT was with one X-Ray beam and one detector that traced the patient in a helical path, providing images with helical scans for the chest, wherewith one breath-hold a continuous scanning for the patient while he is moved through the CT gantry, having very good quality and full scan of the chest cavity [33]. The later edition of CT scans is called (MDCT) multi-detector CT scanner because its detectors were lined in rows of (4, 8, 16, 32, 64, or 128 rows) providing an increase in temporal and spatial resolution scans due to the continuous and rapid data acquisition using thin slices within a single breath-hold. This technique delivers two-dimensional multiplanar reformation images in the coronal, sagittal, or oblique plane, and is called multiplanar reconstruction (MPR) images [34].

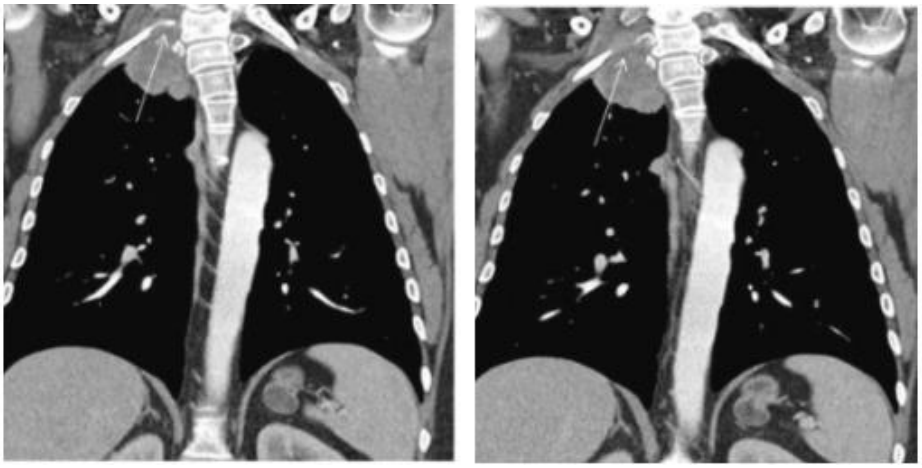

Fig 2.7 Two-dimensional multiplanar reconstruction (MPR) images in coronal planes [34].

Another development has occurred on the CT scans to provides 3-D reconstructions scans, which provides an anatomical overview of the airways, this 3-D rendering of the airways gives images equivalent to bronchoscopy which is called virtual bronchoscopy (VB) that can be used according to Finkelstein et al as a noninvasive method to define bronchial obstructions and endoluminal lesions, where they found that the sensitivity of VB was 100% for detection of obstructive lesions and 83% for endoluminal nonobstructive lesions [35].

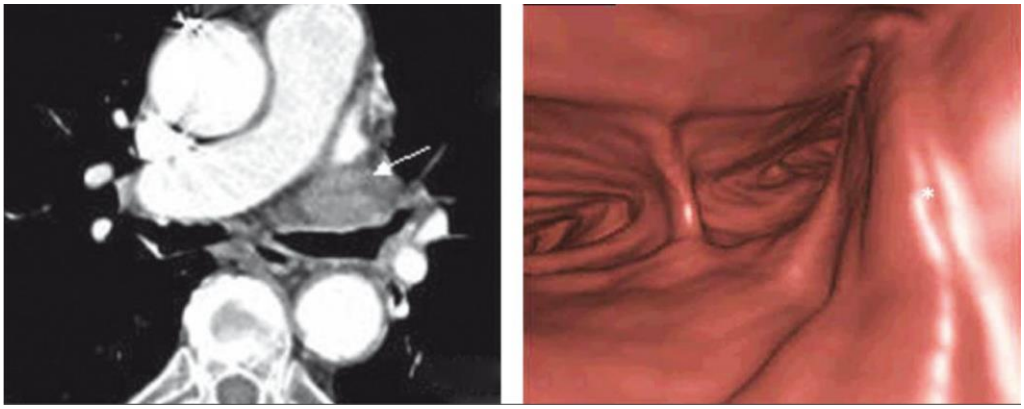

Fig 2.8 CT image and virtual bronchoscopic view [35].

In most cases, VB can depict direct tumor signs, such as a tumoural mass, a wall irregularity, or a loss of cartilages.

2.4.2.3 MR

It is the least used and the most limited imaging technique for lung testing due to the high sensitivity of MR to movement artifacts (i.e. pulsation and breathing), the low proton density of lung parenchyma, and the signal limitations as a result of air–tissue interfaces. Therefore, it is used in addition to CT scans only for specific cases: define the extent of tumor spread in the chest wall and lymphoma in the mediastinal structures "Pancoast tumor" which arises in the lung apex and invades the surrounding soft tissues, distinguish between blood vessels and solid masses, and assessment of diaphragmatic abnormalities [36].

2.4.2.4 Positron Emission Tomography (PET)

Positron emission tomography (PET) is a lung imaging technique that is based on measuring the emitting positron after the patient swallows radioisotopes of natural elements, this technique allows the imaging of metabolic pathways in the human tissue using a PET camera. In thoracic oncology, the radioisotope used is fluoro-deoxy-glucose (FDG) as cells react to it in the same way as glucose allowing them to take up and metabolize it [37] but the malignant cells have higher rates of glucose metabolism than normal cells, therefore it will absorb large amount of FDG which led to positron-emitting that will be traced using the PET camera. After the positron-emitting, It will merge with an electron releasing a pair of photons that will separate each in the opposite direction where they will be detected by the detectors in the PET camera, using these registrations, tomographic images of the regional radioactivity distribution are reconstructed "emission images" [38].

PET/CT is a combined device using both the CT and PET technology, where the CT method provides anatomical information, and the PET technology provides metabolic information, this

combination provides additional information of cancer, such as detection of non-seen Maligns by on CT or PET, the better spatial resolution of Maligns, better characterization of Malignsfrom their surrounding structures, and better delineation of lesions as benign or malignant [39]. The figure below shows the difference between the three methods in imaging lung cancer

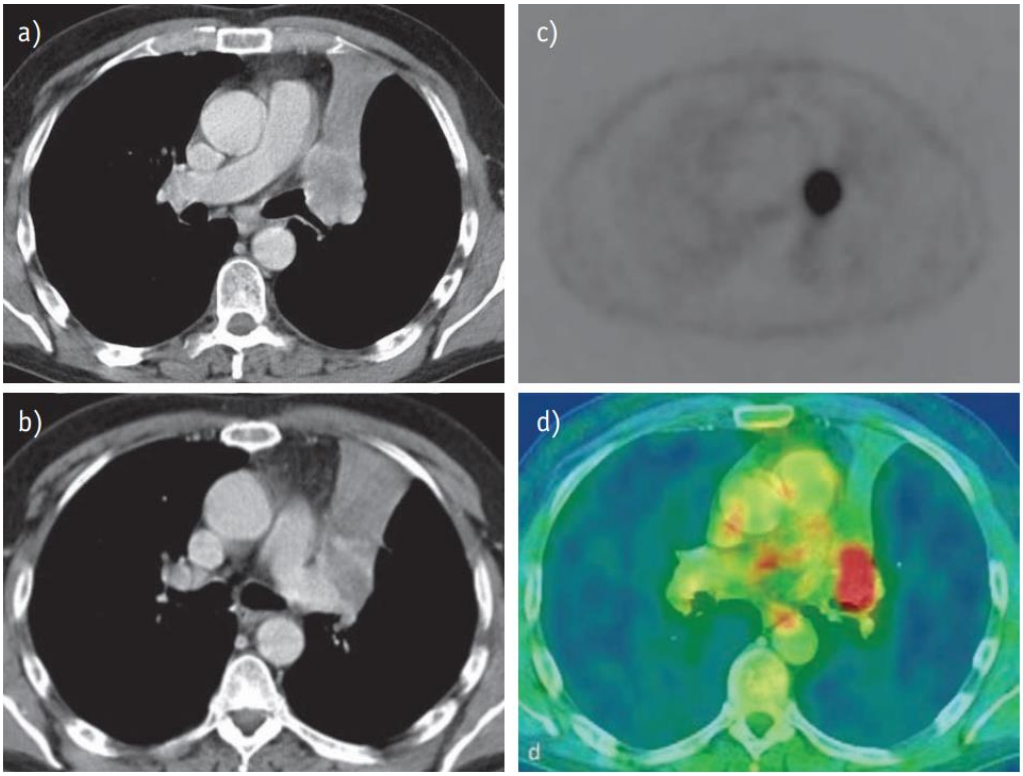

Fig 2.9 CT/PET lung imaging techniques [39].

a–b) Axial CT images showed a central tumor in the left lung. c) PET showed a hotspot in the left lung corresponding with the central tumor. d) Integrated PET/CT imaging showed the hotspot located on the central tumor. it is noticeable that integrated PET/CT provides better tumor discrimination.

Chapter III

Deep Learning

3. Chapter 3: Deep Learning

3.1 Overview

Deep learning is one of the most important aspects of machine learning (ML) taking an emerging area of artificial intelligence (AI) research, it is a computational tool that learns complex motifs from large sequence data sets, comprising multiple hidden processing layers of artificial neural networks to discover structures and patterns in those data sets. This method has improved the state-of-the-art in recognition of speech, image processing, object detection, and many other aspects such as drug discovery and genomics.

The first time when the Deep Learning concept was used was in 2006 as a new field of machine learning and was known as hierarchical learning [39]. Today Deep learning considers two factors in its learning method which are nonlinear processing and supervised or unsupervised learning in order to solve perceptual problems such as image and speech recognition is increasingly making an entry into the biological sciences.

The nonlinear processing in multiple layers is based on a hierarchy algorithm where the running layer takes its input from the output of the previous layer. Hierarchy is an important algorithm among layers to figure out the useful and necessary data to be considered or not. Moreover, supervised and unsupervised learning are related to the existence of the desired target, in the supervised system means there is a target and it works to reach it, while its absence means an unsupervised system[40].

3.2 Deep Learning Architectures

Deep learning has many uses in life aspects, however, it has a variety of usage in medicine especially in medical images by using its architectures and neural networks for Segmentation and Classification to detect and specify many diseases, and many architectures depend on deep learning:

3.2.1 Convolutional Neural Network CNN

It is designed to manipulate data that come in the form of multiple arrays, for instance, 2D images that contain three arrays with three color channels with different intensities, this neural network uses four factors which are local connections, shared weights, pooling, and the use of many layers. Where its structure is composed of series of stages, the early stages contain two

kinds of layers convolutional layers and pooling layers. In a convolutional layer, there are units organized in feature maps, each patch is connected to the previous layer specifically to the local patches in the feature maps through a set of weights called a filter bank, then the weights will be summed and passed through a non-linearity such as a ReLU. All units in the same feature map have the same weight, and it will be different if there is a change in the feature maps.

$$Z = W.X + b \qquad (1)$$

Where: W is the wight, x is the unit and b is the bias

the idea of units that share the same wights even if they are in different locations comes from if a motif can locate in a part of the image, it could show anywhere of the image which allows to detection of the same pattern in different parts of the array. while the role of the pooling layer is to merge semantically similar features into one creating what is called by patch, then it will compute the maximum of a local patch of units in one or a few feature maps. multi stages will be made that have the same order of convolution, non-linearity, and pooling layers followed by more convolutional and fully-connected layers to backpropagating gradients through a ConvNet regular deep network, which will allow training all the weights in all the filter banks[41]. This architecture is used in both segmentation and classification and showed a very high accuracy to get its target.

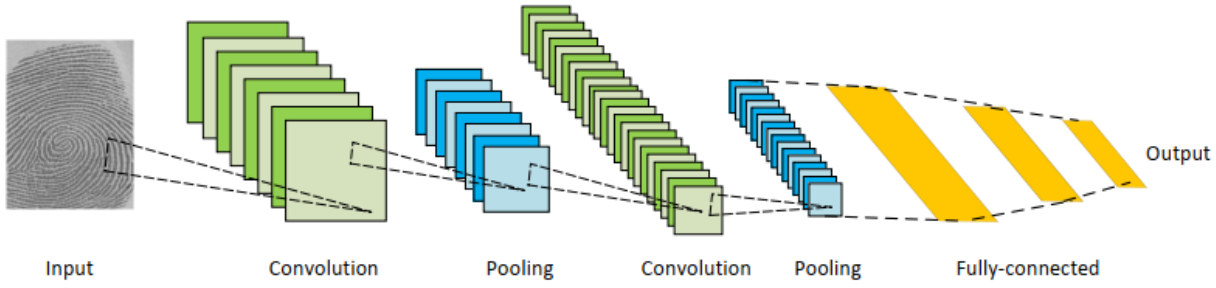

Fig 3.1 Architecture of convolutional neural networks

3.2.2 Recurrent Neural Network RNN

It is one of the most widely used neural networks today especially for tasks that involve sequential inputs such as image processing because RNNs not only evaluates their inputs instantly but also its evaluation depends on the past inputs, RNNs process an input sequence one element at a time with keeping a 'state vector' in their hidden units where the state vector has information about the history of all the previous elements of the sequence [41], and this is

the key feature of an RNN having feedback connections that allow the RNN to apply the effects of the earlier parts of the sequence on the later part of the sequence [42].

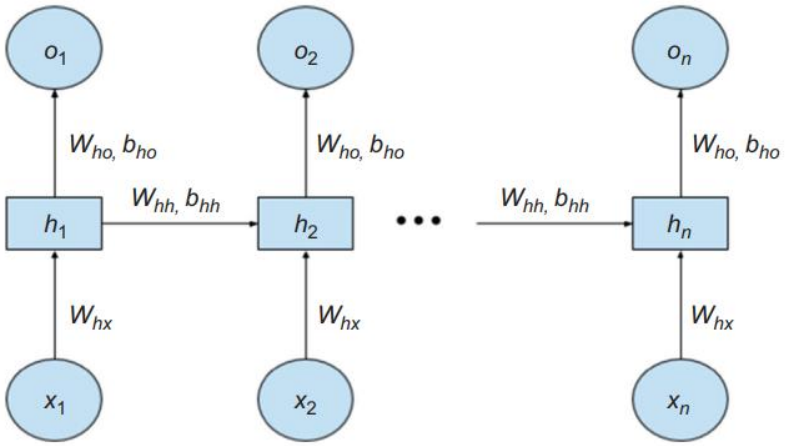

Fig 3.2 Architecture of Recurrent neural network

RNNs can be “unfolded” in time and trained using backpropagation through time, where all the layers share the same weights across multiple timesteps and are updated. even though the main aim is to learn in long-term but theoretically and empirically it is difficult to learn information storage for very long [43], this problem has been solved by augmenting the network with an explicit memory using long short-term memory (LSTM) network that has its memory cell that can save some information about the sequence to remember the inputs for a long time that might affect the later parts of the sequence, that is by using also the important features at the beginning of operation without calculating the output based on just the previous time step. LSTM has three gates: the input gate, the forget gate, and the output gate. The input gate has to control the inflow of new information, and the forget gate will control the memory, “i.e. it will decide if there is some information that should be dropped or not" and make a space to store new information. The output gate will control when the information is used in the output from the cell [42].

3.3 Applications

Deep learning is using today in many real-life aspects such as digital image processing; where the machine can color a grayscale image from a picture made by users manually who will choose each color based on their preferences, or adding sound into a video using Recurrent Neural Networks (RNN), in other words, this state-of-the-art has improved the results and optimized the processing times in several computing processes. In the field of natural language

processing, deep learning methods have been applied for image processing, and handwriting generation and recognition [44].

3.3.1 Image processing

it is one of the deep learning applications, wherein 2003 an application has been improved with filtering and Bayesian – belief propagation, and the main purpose was allowing the humans to recognize a face by watching only a half–cropped face picture, then use this picture to rebuild the full-face image by computer [45]. Many other applications have been made using deep learning and its architectures like using CNN for Iris Recognition where CNN accuracy can reach up to 99.35 % [46]. Nowadays many applications like Google, Facebook, and Microsoft are using deep learning for face recognition, moreover, Sighthound Inc. has developed a deep convolutional neural network algorithm to recognize also the emotions from images besides age and gender, where for face recognition, neural networks follow different ways to get the exact results, one of them is by using the images as an input for the first hidden layer to extract some features like edges and do further more complex processing in the next subsequent layers, which make finally a decision to recognize the human face at the final layer. Furthermore, a traditional approach is also used by applying a pre-processing on the image by experts as the first step for features extraction followed by automatic manipulation using a neurla network arctiecture to get the final result [47].

3.3.2 Medicine

Digital image processing played a very important role in the research fields where a deep learning method can be applied. For example, the comparison between shallow learning and deep learning in neural networks enhanced the performance of disease prediction. Today, images are taken with MRI or CT from lungs, brain, Iris, or any other human parts to be processed in order to predict possible diseases such as cancer or Alzheimer's. but there are some limitations in training depending on the high volume, quality, and complexity of data, however, the integration of heterogeneous data types is a potential aspect of deep learning architecture [40].

3.3.3 Lung cancer segmentation and classification.

As chest radiography is still the most commonly used imaging modality for screening a large number of pulmonary diseases. and what makes it very popular, that It is fast, easy, non-invasive, and inexpensive, and is thus widely available in emergency rooms. Although easy to acquire, a chest radiograph is one of the most complex imaging modalities to explain. where many physicians in an emergency room make many mistakes in reading radiographic, besides

the differences between their interpretations and the radiologists' interpretations. This makes using developed computer-aided diagnosis (CAD) systems to make decisions is highly desirable that can automatically interpret and assist medical practitioners in decision making [48]. many CAD systems have been developed over the last years, providing very important techniques making chest radiographic is easy to understand and explain by extracting features from the images and using them for segmenting anatomical structures to define region-of-interest (ROI) and classify the type of pulmonary disease [49]. Lung cancer segmentation and classification has attracted the considerable attention of many researchers who developed many techniques to get the best result and accuracy in reading images, and deep learning as a technique plays today a very important role where it is considered the state-of-the-art in image processing field. Many architectures have been developed to analyze and understand medical images such as CNN and RNN which are automatic, hierarchical methods with multiple levels of abstraction, and more closely resemble the way it is done by the human brain. Neural networks are considered deep network when their structure contains more than 2 hidden layers of neurons and greater than 10 is very deep networks. Those nìhidden layers use the image features like pixel-wise, gray- scale and the whole dataset volume to build make feature map that acts as input for the neural network in order to segment Roi from the image and classify the cancers type in the lung[49].

Chapter VI

Literature review

4. Chapter 4: Literature review

4.1 Segmentation

Image segmentation is the process of apportioning digital images into multiple parts with a straightforward approach. it is utilized to distinguish the object (or) other related data, and segmentation aims to simplify and (or) potentially change the representation of an image into something more important and easier to analyze. Image segmentation is typically used to locate objects &boundaries (lines & curves) in images [50].

Image segmentation plays a very important role in the medical aspect providing valuable information about diseases. in the last few years, many researchers work on understanding cancers using image segmentation, for example, lung cancer, as figure (4.1) below, shows the improvement of the number of researches about lung cancer segmentation through the years, where the first research in this field began at the beginning of the first decade of this century with a very few numbers but it started to improve through last years due to the increasing understanding of medical images and the development of image processing and segmentation methods. Also, with the emergence and development of neural networks

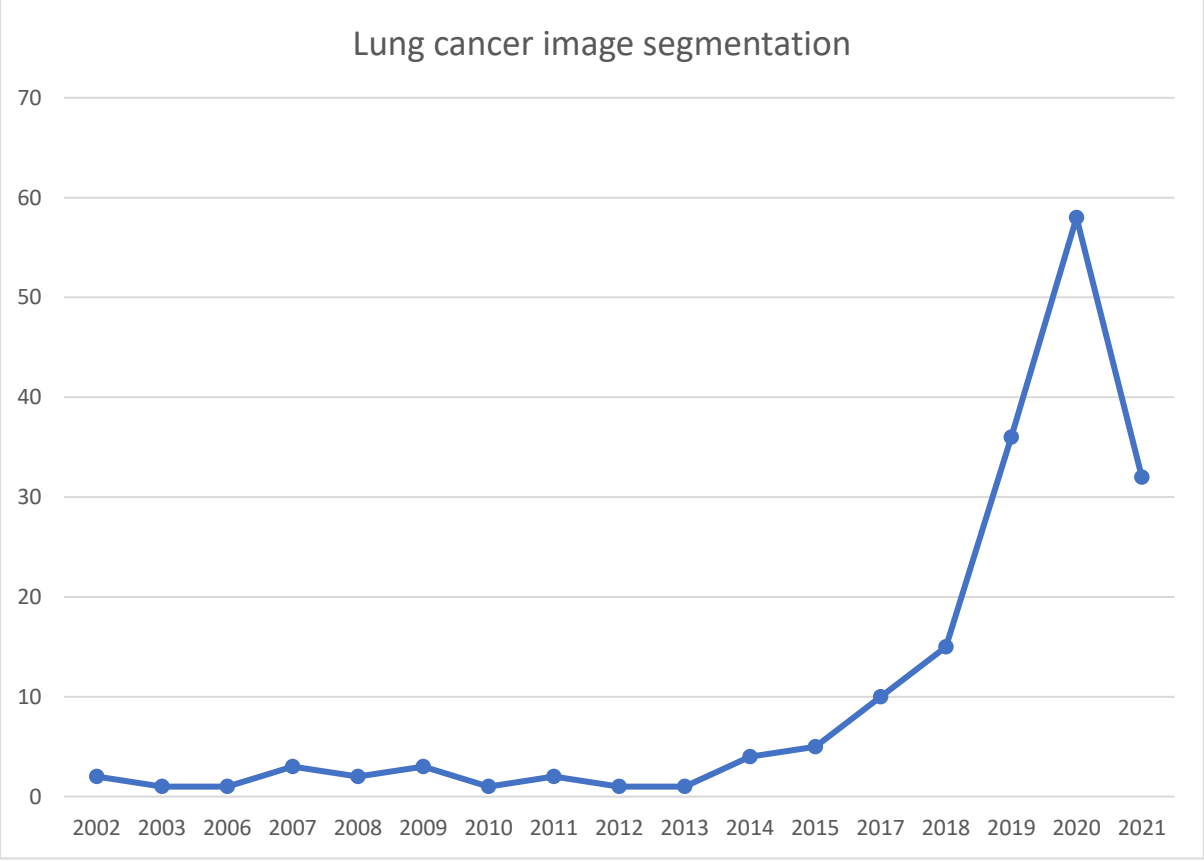

Fig 4.1 increasing lung cancer segmentation research through years [51]

the figure above shows the results of searching for lung cancer segmentation using research engines which is PUBMED which shows about 100 results in the last 4 years while by using the google scholar it shows more than 180 researches and IEEE shows about 132 papers some of those papers did not use machine learning for the segmentation while they different strategies for segmentation, including thresholding, wavelet, region growth, active contours, and watershed methods. For this reason, another keyword was added for the searching which is lung cancer segmentation using neural network and we have selected, the results of this search in the figure below which is an explanation of this step.

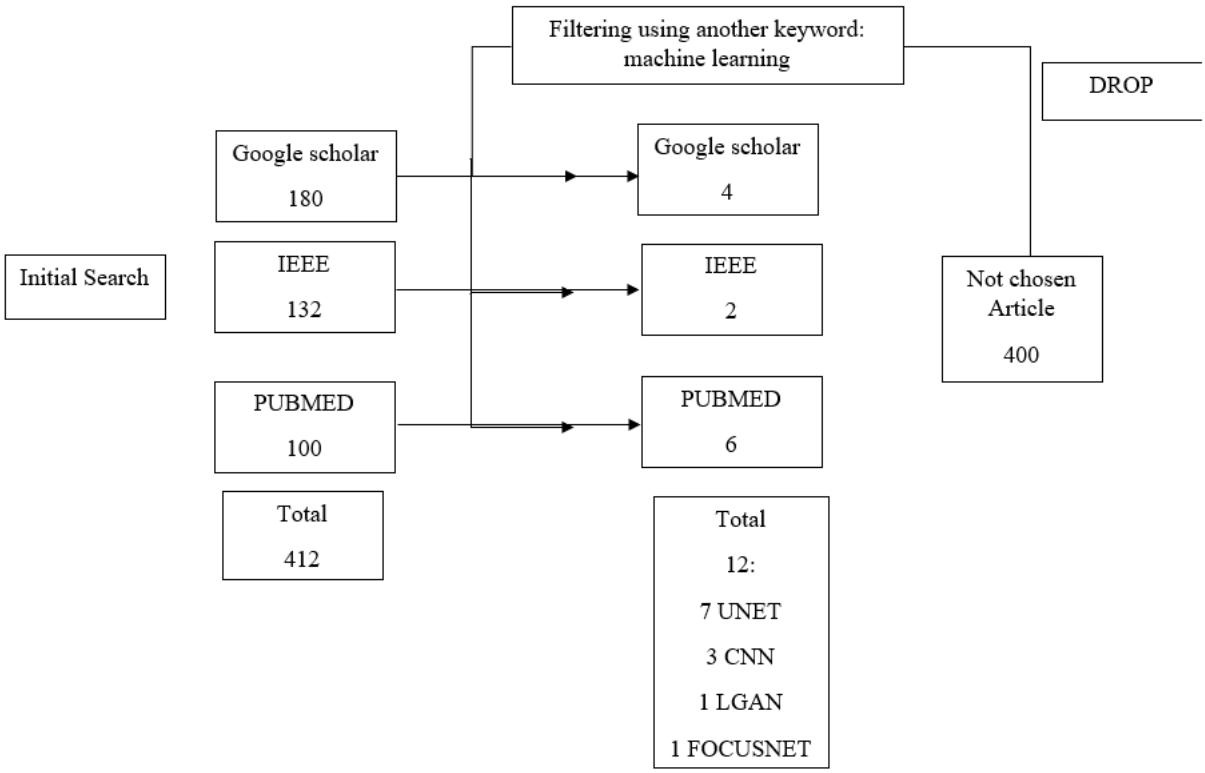

Figure 4.2 search engine approach for lung cancer segmentation

Ref	Data acquisition	Number of Patients	Number of slices	Resolution	Confounders	Input	Segmentation method	ACC %	Se %	Sp %	AUC %
[52]	CT	1	267	128×128 resized to 32x32	Chest cavity Irregular-boundaries	Gray-level density	2D-U-net	96.78	NA	NA	NA
[53]	CT	1	NA	NA	Surrounding area	Cropped images	2D-U-net Deep Learning	95	NA	NA	NA
[54]	CT	1	4,121	512×512	NA	Original CT images	2D-CNN	97	1.0	94	97
[55]	CT	39	333	512 x 512	Slow detection speeds Large memory usage Noise	lung density	2D- Mask R-CNN	97.68	96:58	97:11	NA
[56]	CT	377	(460-1177)	128×128×4	NA	3D Set of CT images	3D FCN (3DUnet)	89.4	NA	NA	NA
[57]	CT	1	1,012	64×64×64	NA	Images with K-Kernal	3D- UNet++	NA	NA	NA	NA
[58]	CT	888	NA	NA	Proplem in training due the large layer's number	CT image	3D-Res2UNet	95.3	99.1	NA	NA
[59]	CT	267	NA	Resampled to 32x32	NA	CT image	2D- FOCUSNET	99.32	97.57	99.81	NA
[60]	CT	220	130	512×512	Noisy masks, mode collapse	Grayscale	2D - LGAN	NA	NA	NA	NA
[61]	CT	23 201	2460 19,967	512 × 512	Patches of background air	Image patches	2D- CNN	99.2	98.8	99.5	99.91
[62]	CT	NA	NA	512 × 512	Noise	Pixels features, grayscale	2D- Random Forest	98.67	NA	NA	NA

[63]	Biograph 40 PET/CT	60	112 - 293	512 × 512	Outliers	Voxel Features	2D- U-net	NA	NA	NA	88

Table 4.1 Research review of lung cancer Classification using neural networks

Shaziya et.al in 2018 [52], used U_net architecture in order to segment the lung by inserting the lungs dataset that contains 267 CT pictures with size 128x128 then and the first step was applying a resize of those images into 32x32 pixels, the dataset is divided into training and test sets in proportions of 70% and 30%, respectively. Rotation operation is used to augment training samples. Every training sample has eight different rotating versions of itself. The U-Net ConvNet is made up of many layer blocks that move in a contracting and expanding direction. The augmented dataset is used to define the input layer at first. Followed by a Con1 layer that requires eight 3x3 filters, and the image's size remains the same. This Con1 has a connection to another con1. In the complete network, con layers are followed by relu. Then there's pool 1, which is 2x2. Pool1 shrinks the image to 16x16 pixels. Con2 employs a total of 16 filters, then Pool2 enlarges the image to 8x8 pixels, after that a Pool3 changes the size to 4x4 and con3 contains 32 filters. It was a contracting course until pool3. Con4 marks the start of the expansive road. Con4 is a concatenation of con3 and has 32 1x1 filters. Concat is followed by upsampling up1, resulting in an image size of 8x8. Con5 is made up of 32 filters that have been concatenated with con2. The size is changed to 16x16 by Up2. Con6 is made up of 32 filters that have been concatenated with con1, then the size is increased to 32x32 by Up3. Con7 features 16 filters, while Con8 has 64. In con5, con6, and con7, the filter size is 2x2. The size of the Con8 filter is 1x1. After con8, there is a dropout. The output layer has one 1x1 filter and works with images up to 32x32 pixel as shown in the figure below which explains their architecture, With an accuracy of 96.78 percent, their model's output is close to the ground truths.

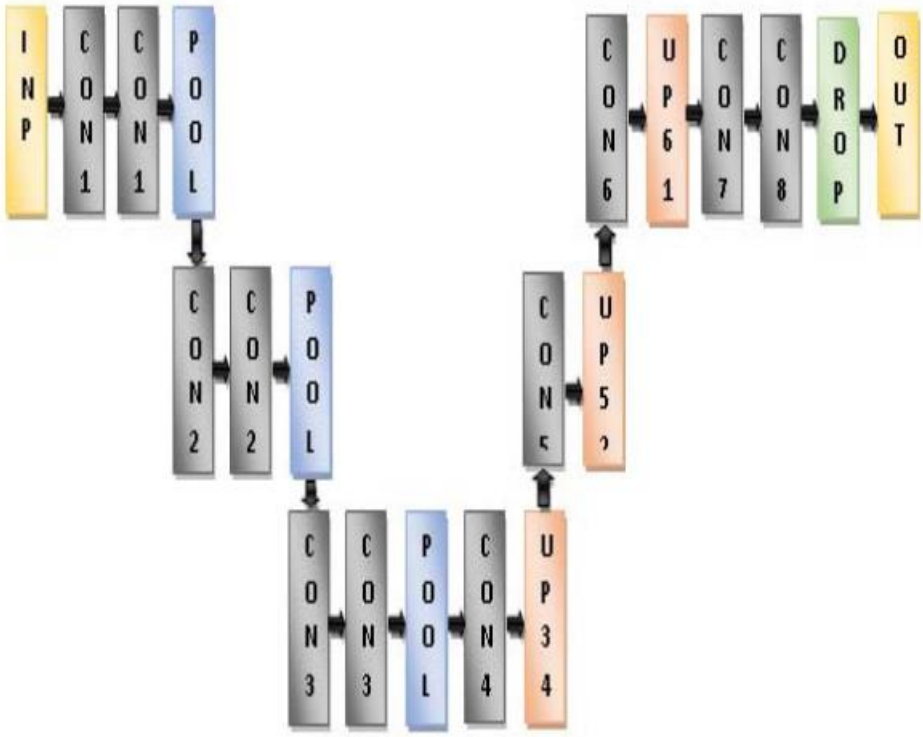

Figure 4.3 Shaziya et.al architecture [52].

Hassani, E L and et.al in 2018 used Unet model for lung segmentation where their architecture consisted of two paths: the left path, which consists of two convolutions with the same padding followed by ReLU and a 2x2 max-pooling with stride 2, and the right path, which consists of an up-convolution of the feature map from the left side and two 3x3 convolutions followed by ReLU, and this operation is repeated four times. Due to the loss of border pixels in convolution layers, it was necessary to crop and concatenate corresponding feature maps from the left side with their corresponding feature maps in the other path as shown in Figure 4.2, they utilized the input images and their respective masks to train the U-net in the training phase, and used an image as input to create the corresponding mask as output in the test phase. The mask is then applied to the relevant image to segment the area of interest, which was the lung parenchyma. But before starting the training and using the U_net they applied a manual segmentation that gave the ground truth for the lung parenchyma, and they undertook a pre-processing step that consisted of cropping the images to simply remove any information that didn't belong to the research area. They could achieve an accurate segmentation with a Dice-coefficient index of 95.02 [53].

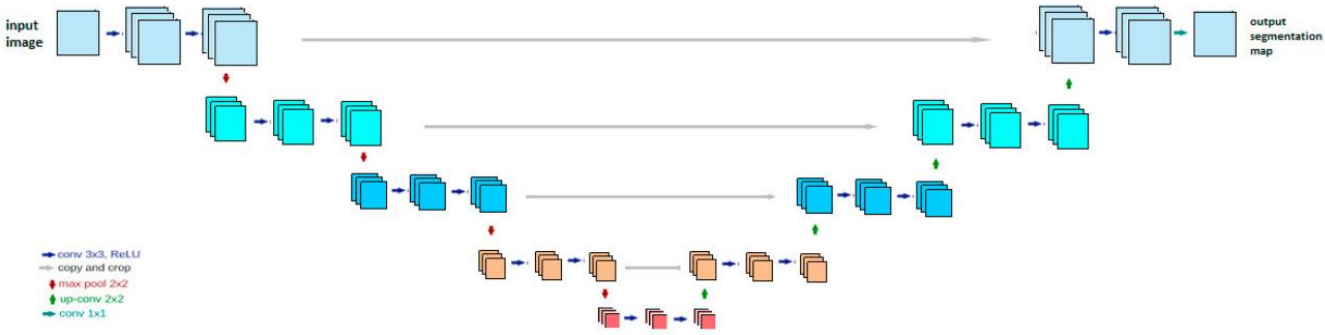

Figure 4.4 Hassani, E L and et.al architecture [53]

Men et al. proposed 2D-CNN for lung cancer segmentation, where their dataset provided by the small gold standard atlas from the Lung CT Segmentation Challenge 2017, which contained 36 cases, and 110 cases from the NRG Oncology/RTOG-1308. Their method consisted of five steps and was based on automatic segmentation with deep active learning: For the illness location, they created a gold standard atlas and separated the clinical trial cases into candidate, validation, and test sets. and by despite the fact that the gold standard atlas did not represent a huge population, they used it to train the CNN segmentation model. To compensate for the model's lack of training data, they choose high-quality photos from the candidate set to add to the training set for fine-tuning. The images were chosen based on their representativeness, which was determined using a parameter that combined uncertainty and accuracy. Then they tested the fine-tuned model's accuracy by applying it to the validation set, which included contours that were proved to be accurate. The Dice similarity coefficient (DSC) and the Hausdorff distance (HD) were used as evaluation measures. The QA criteria were then established using these metrics. Finally, they ran the test set through the fine-tuned CNN model and the decision criteria to see if any of the contours were incorrect. they used a CNN in order to have a state-of-the-art performance. The set of original CT images served as the CNN's input, and the matching segmentation probability maps for the OARs served as the CNN's output. And they used general data augmentation methods including random scaling (from 0.5 to 1.5), random cropping, and random rotation (-5° to 5°) to avoid overfitting. The model best values were accuracy 97%, sensitivity 100%, specificity 94%, and AUC 97% [54].

Roth et al. in [56] created a 3D U-net model derivative from 3D-FCN for CT scans segmentation, where their model started by two kernel convolution layers followed by RELU activations then followed by max-pooling, they used smooth B-spline deformations to both the picture and label data in training, comparable to. The deformation fields are chosen at random from a uniform distribution with a maximum displacement of 4 and a minimum displacement

of 0. This method of data augmentation can artificially increase the training data and encourage convergence to 20 to +20 voxels in each dimension at each iteration to generate convincing deformations during training. The voxels are separated by a 24 voxel grid. We also used random rotations of 20° to +20°, as well as translations of more robust solutions, to reduce overfitting to the training data. And their method for feature extraction was repeated to downsample the scan to 3x3x3 then upsampling. by learning a highly sophisticated non-linear relationship between the two paths from the images to the segmentation The 3D U- ReLU activations and a 2 x 2 x 2 max pooling with two-dimensional strides. The analysis path has two convolutional layers with 3 x 3 x 3 kernels each, followed by Net architecture consisting of symmetric analysis and synthesis paths with four resolution levels each. Each ReLU is activated. Furthermore, 3D U-Net makes use of shortcut (or skip) connections between layers of equal resolution in the input images' space. These are followed by two 3 x 3 x 3 convolutions, each of which uses posed convolutions to remap the network's lower resolution feature maps to the higher resolution feature maps. Their work has been achieved with accuracy reached to 89.4 %.

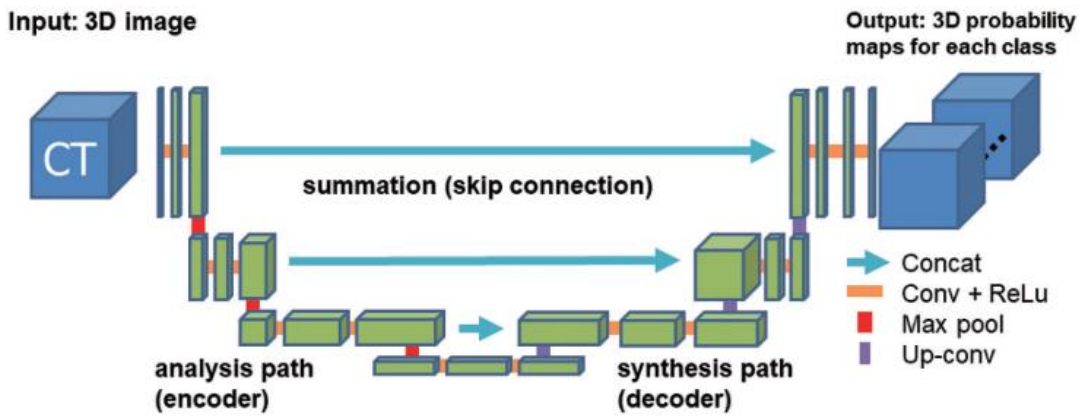

Figure 4.5 3D_UNET architecture [56]

Zhou et al. in [57] proposed Unet++ architecture for lung nodule segmentation based on nested and dense skip connections, their model started with an encoder sub-network or backbone followed by a decoder sub-network, then the re-designed skipped pathways that connected the two sub-networks and the use of deep supervision is what , as well as the application of deep supervision, distinguish UNet++ from U-Net. UNet++ is made up of an encoder and a decoder linked by a sequence of nested dense convolutional blocks as shown in the figure 4.6.Where The main idea behind UNet++ is to bridge the semantic gap between the feature maps of the encoder and decoder before fusion.

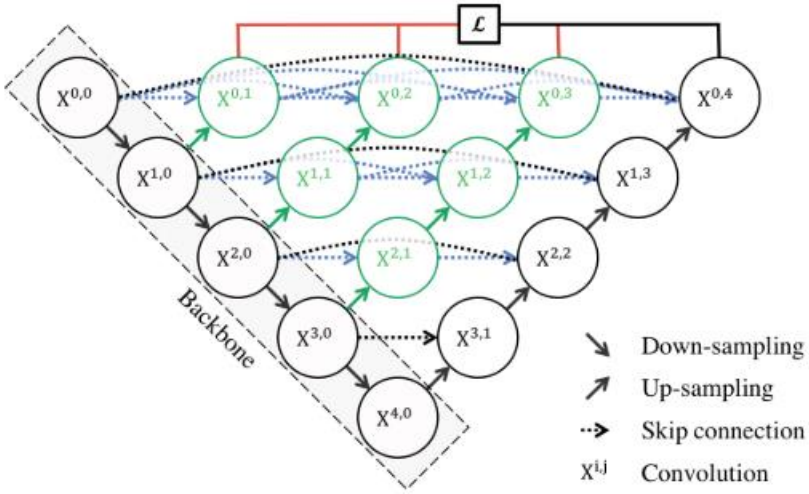

Figure 4.6 U_NET++ Archetecture [57]

Xiao et al in [58] proposed 3D-Res2UNet architecture to segment the lung nodules from CT scans, which is composed of 3D-UNet and Res2Net, which contained 23 layers. The features have been extracted using down sampling and the combination between U-net and Res2Net allowed to capture of very small features. This method achieved a good result in the segmentation with where the dice coefficient index reached 95.30% and the recall rate that referred to sensitivity reached 99.1%.

Kaul et al. 2019 in [59] proposed FOCUS-NET neural network to segment lung cancer from CT scans and skin cancer with RGB CT scans, where they down sampled their input using stridden convolutions rather than max-pooling then up sampled, their methods segmented lung cancer with an accuracy of 99.32%, sensitivity 97.57%, and specificity 99.8%, and for skin cancer showed accuracy 92.14%, sensitivity 76.73%, and specificity 98.96%.

Their method based on Attention is used in the network architecture to provide improved per-pixel predictions, resulting in better segmentation. The two branches are encoder-decoder structures in which the per-layer decoded output is multiplied with the output of the first SE block using a sigmoid gating function.

And for downsampling Instead of employing max pooling, strided convolutions are used for that. The result is a per-pixel prediction from a 1x1 convolution with sigmoid activation. The receptive field of the remaining convolutions is 3x3. The filter bank volumes that were employed were 32 – 64 – 128 – 256 – 512 – 256 – 128 – 64. The use of skip links throughout the architecture improves gradient flow, making it easier to train a deeper network. In addition,

SE blocks are frequently employed to reweight the output feature maps at intermediate steps. We employ a fixed rate of dropout for hyperparameter settings.

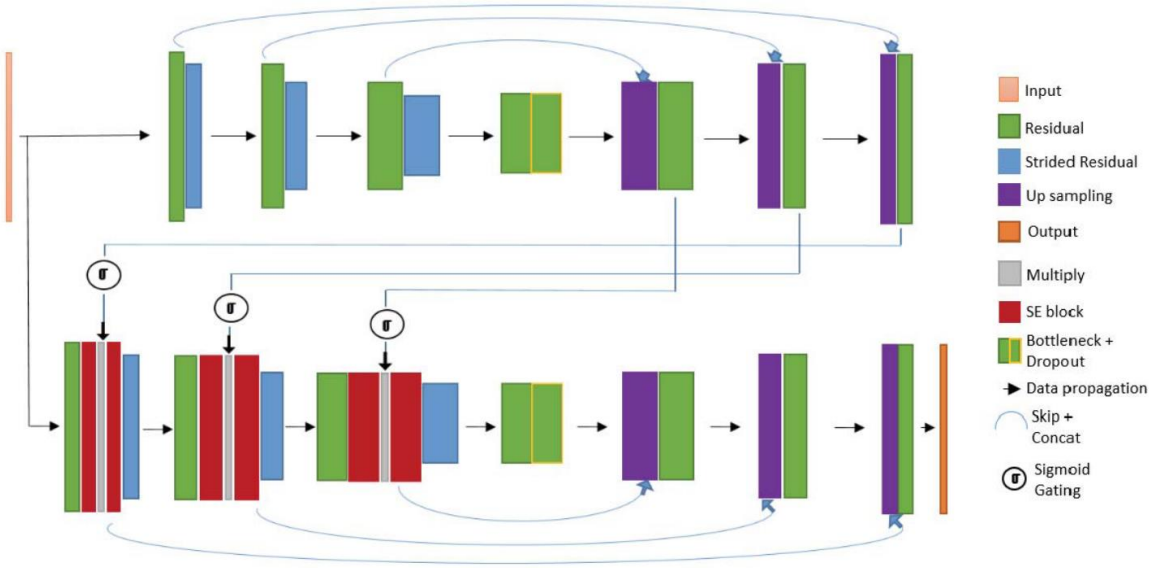

Figure 4.3 FOCUS-NET architecture [59]

In [60] 2021, Tan et al. proposed the LGAN model to segment the lung from CT scans based on Generative Adversarial Network structure, where the neural network is trained to generate the lung mask based on the grayscale, and the Adversarial Network is trained to discriminate segmentation maps from the ground truth and the generator.

Xu et al in [61] proposed 2D -CNN neural network to segment lung parenchyma from CT scans. They split CT scans into image patches, which used as an image input layer, followed by a convolutional layer, a pooling layer, and two fully linked layers with a Softmax layer make up the construction of this CNN network. As shown in figure 4.4 .then performed a clustering algorithm with two categories twice, to generate more accurate lung parenchyma boundaries combination with a mean intensity of patch and the cross-shaped verification the result used as input for the model that segment the lung parenchyma with accuracy up to 99.2%, Sensitivity = 98.8%, Specificity= 99.5%, and AUC = 99.91% .

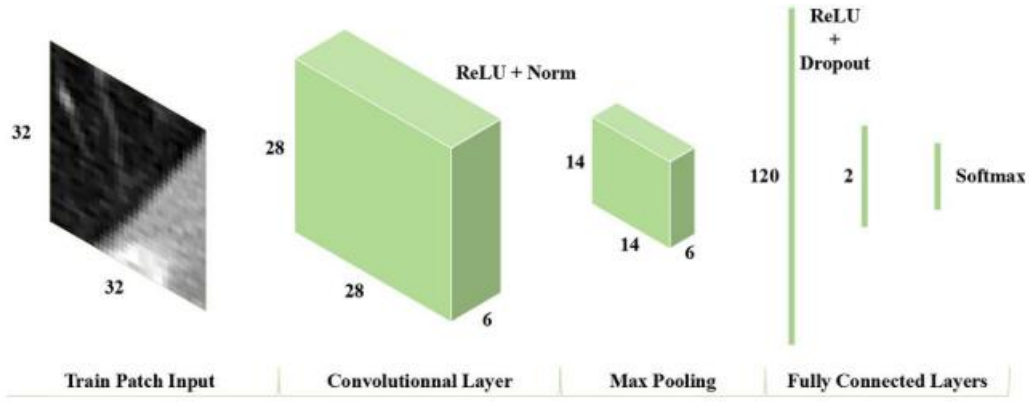

Figure 4.4 CNN architecture [61]

Liu et al. 2020 in [62] proposed Random Forst model for lung cancer segmentation from CT scans, their algorithm consisted of five main steps: 1- image preprocessing "by using normal vectors to measure the similarity between two image blocks and then construct a novel normal vector correlation-based image denoising (NVCD) approach", 2-lung region extraction following "multi-scale decomposition, superpixel segmentation, feature extraction, and superpixel classification", 3- trachea elimination "where the intensity of the trachea is always homogeneous, compared with that of the lungs so the iterative thresholding was a suitable method to segment tracheas",4- lung separation "based on a context supervising interpolation technique", 5- contour correction based on "a corner detection strategy". Their work showed in segmentation the lung cancer an accuracy result = 98.67%

In 2019 Baek et al [63] proposed U-net neural network for lung cancer segmentation on PET/CT scans where they entered three-dimensional (3D) volume image as an input and used the "bottleneck layer" technique to process the images, where the image features are compressed, and reconstructs the image into a binary segmentation map indicating a pixel-wise tumor classification result. Their work results showed an AUC = 88% for lung cancer segmentation.

4.2 Classification

classification is the problem of identifying to which of a set of categories (sub-populations) a new observation belongs, based on a training set of data containing observations (or instances) whose category membership is known. An algorithm that implements classification, especially in a concrete implementation, is known as a classifier.

As the segmentation, Also medical image classification consider as a new scientific approach that improved recently due to the improvement of the neural networks, otherwise, it is noticeable that there are some researches that made in the last decade of the 20th century where the specialists used to classify the images manually and based on their experience, for that we can say that classification consider as an older process than segmentation, and there are more researches about it recently for this reason.

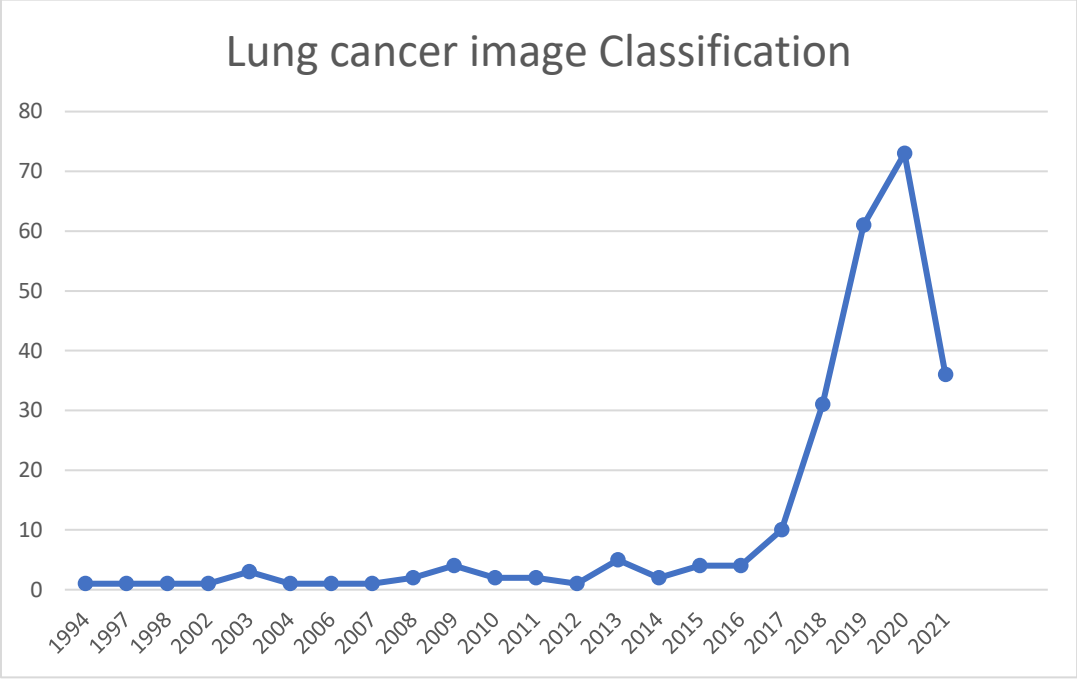

Fig 4.5 increasing lung cancer classification research through years [64]

this figure explains how many researches have been published in PUBMED related to the lung cancer classification by searching in the PUBMED engine and resulted in about 210 research, while in another engine such as google scholar that showed 200 research and in IEEE showed 180 must of those researches were using a different algorithm for classification such as combining grayscale and binary texture features [65]

for that, another keyword used to filter the results with only a machine learning algorithm which was: lung cancer classification using a machine learning model, figure 4.6 explain the search step

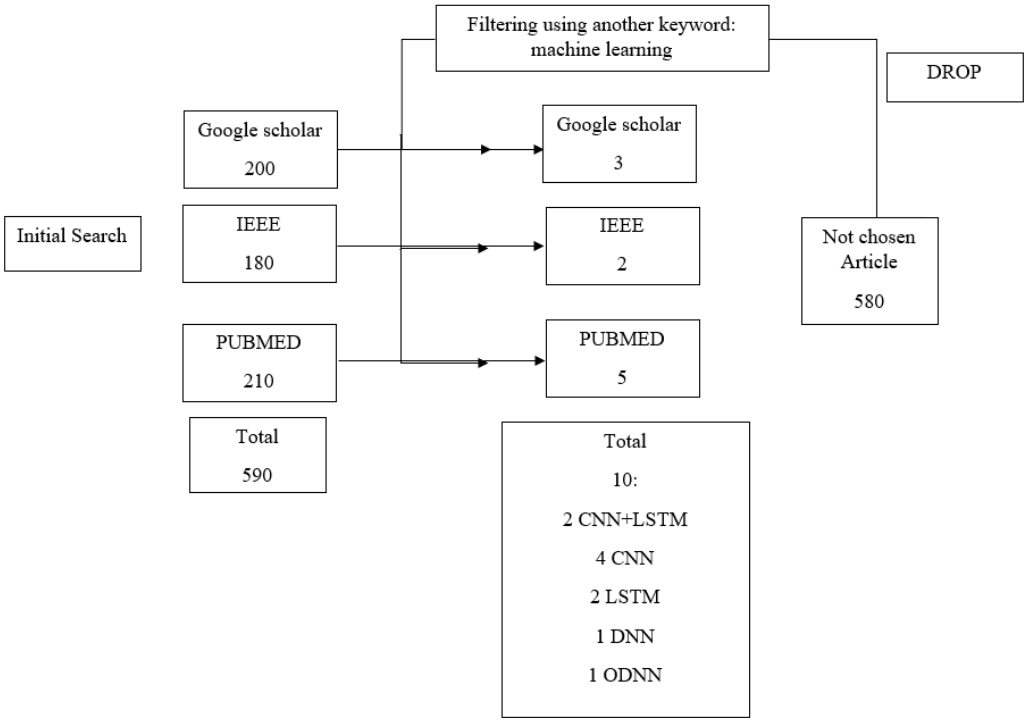

Figure 4.6 search approach for lung cancer classification

Ref	Data acquisition	Number of Patient	Number of slices	Resolution	Confounders	Input	Classification method	Acc %	Se %	Sp %	AUC%
[66]	CT	1010	244,527	NA	Noise and using DICOM Images	grey-scale image	2D-CNN and LSTM	97	NA	NA	NA
[67]	CT	1794	NA	128×128×128	NA	3D volume scans	3D-Distance LSTM	78.96	NA	NA	82.55
[68]	CT	92	16220	32×32	No distinct visual structures, small number of training samples and over-fitting	Image patches	2D-CNN	>90	NA	NA	NA
[69]	CT	NA	100	NA	Noise and bad extracted features	histogram, Texture, and wavelet features	2D-ODNN	94.5	96.2	94.2	NA
[70]	CT	1397 888	100-400 100-400	512×512 512×512	Poor result preprocessing	segmentation, normalization, downsampling, and zero-centering for 3D CT scan	3D-CNN U-Net	86.6	NA	NA	83
[71]	CT	888	226,589	512×512×512 and reseized to 64×64 ×64	surrounding area of ROI	3D CT scan	3D-CNN with 3D Convolutional LSTM	97.2	NA	NA	NA
[72]	CT	2101	NA	512×512	NA	3D images	3D-CNN + SVM	91.8	88.5	94.2	NA
[73]	CT	6648	8794	128 × 128 × 35	NA	CT images	3D- LSTM	NA	77	74	83
[74]	CT	NA	NA	NA	image quality	Set of Gray-level co-occurrence matrix (GLCM), and Gray-level Run Length Matrix (GLRLM)	DNN	95.2	86.4	100	NA
[75]	CT	311	NA	50×50	over-fitting, and small sample size	grayscale images	2D-CNN	76.5	31.3	97.1	71

Table 4.2 Research review of lung cancer classification using neural networks

Mhaske. D et al. in 2019 [66] they proposed LSTM neural network to classify lung cancer combining it with CNN neural network which extracted the features from the 2D images. The CNN architecture contained 22 hidden layers; those images had been pre-processed before entering the CNN by converting from DICOM to .png or .jpeg. which were easier to understand than DICOM, removing the noise with Median filter, then applied one of the segmentation methods which was the thresholding based on the grey-scale of the images using Otsu threshold. The LSTM was the last layer of the CNN -LSTM. The LSTM consists of four gates. Which are input gate, forget gate, output gate, weights, and bias for the respective gates, in order to map the extracted features from the previous layer. figure 4.7 shows the followed architecture. The accuracy of this method was 97% in classification between normal and cancer cases.

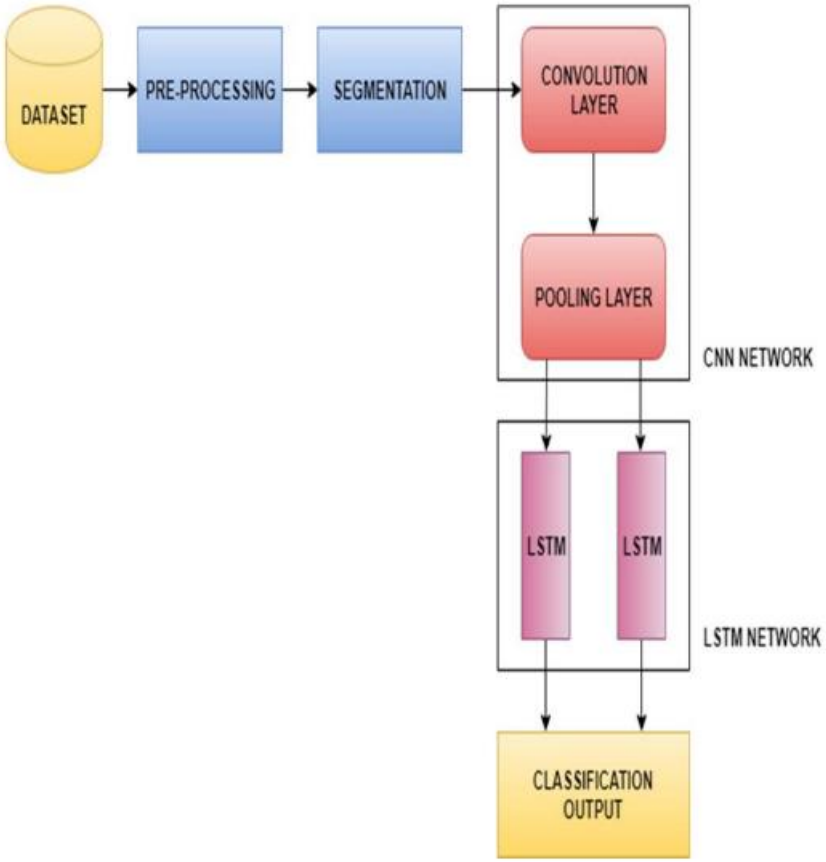

Figure 4.7 CNN+LSTM architecture [66]

In [67], proposed Distance LSTM with two different datasets as a neural network to classify lung cancer from scans acquired from CT, where three gates distinguish the LSTM architecture "forget gate, input gate, and output gate" and the authors incorporated the "distance attribute" to LSTM to get the Distance LSTM by multiplied the forget gate and the input gate with learnable parameters to a Temporal Emphasis Model (TEM) which act as a multiplicative function, their method showed 78.96 and 82.55 for accuracy and area under the curve AUC in the first dataset, 86.97 and 86.97 for accuracy and area under the curve AUC in the second dataset.

Cai et al. in 2014 [68] proposed a feed-forward CNN neural network to classify lung image patches with interstitial lung disease (ILD), the authors built their network with 5 different layers where the input as a normalized lung image patch with unit variance and zero mean. A convolutional layer with a kernel size of 7x7 pixels and 16 output channels is the first layer. A max pooling layer with a kernel size of 2x2 is the second layer the following three layers are fully connected neural layers with 100-50-5 neurons in each layer as shown in figure 4.8, and Relu activation was their method to improve the classification performance by 2.5%. The accuracy of this method was more than 90% in the classification of interstitial lung disease (ILD).

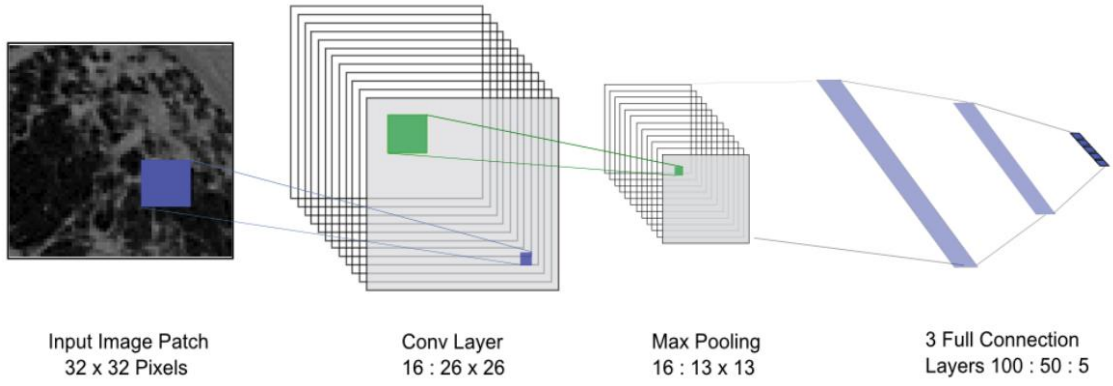

Figure 4.8 Cai et al CNN archetecture [68]

Lakshmanaprabu et al in [69] proposed ODNN architecture to classify the lung CT scans into Normal, Benign, or Malignant, their architecture input was features extracted by the histogram, texture, and wavelet of the image. They used Linear Discriminate Analysis "LDA" to reduce the features to reduce the computational time and cost of our classifying Method. The accuracy

method raised to 94.56% and the sensitivity and specificity were 96.2% and 94.2% in the classification of lung cancer.

Alakwaa et al [70] proposed two architectures to classify the lung cancer "U-net and 3D-CNN", they used thresholding for initial segmentation to segment the lung from CT scans and feed them into 3D-CNN for classification which contained 2 convolutional layers for feature extraction and one fully connected layer for classification a shown in the diagram below, another input was provided to CNN from a modified U-net which detected the nodule from CT scans, this approach provided a classification accuracy of Lung Cancer with 86.6% and AUC with 83%.

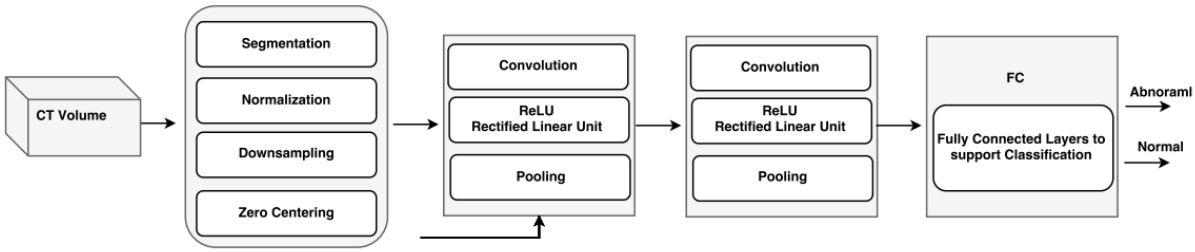

Figure 4.9 Alakwaa et al architecture [70].

Olulana et al 2020 [71] proposed a hybrid algorithm for nodule generation of Lung from CT scans composed from CNN with 3D Convolutional LSTM algorithm where the LSTM archetecture built as Wh is the shared weight matrix for the hidden-to-hidden transitions at time step τ, Wx is the shared weights for the input-to-hidden connections, as well as Wpeep is the shared weights matrix for the peephole connections. The b is the bias, as well as C(0), h(0) are the initial states of the memory cell and the hidden state, respectively. Furthermore, one of the batch-normalization (BN) layers with its learned shift; γ and scale; β, are denoted by (x; γ, β) where the bias terms are denoted by b as shown in the figure 4.11, and the CNN used for features extraction. The authors produced a 3D tensor that flows through each cell by convolving the input and the previous hidden states, their method achieved 97.2% as accuracy for detection of the progression of lung cancer.

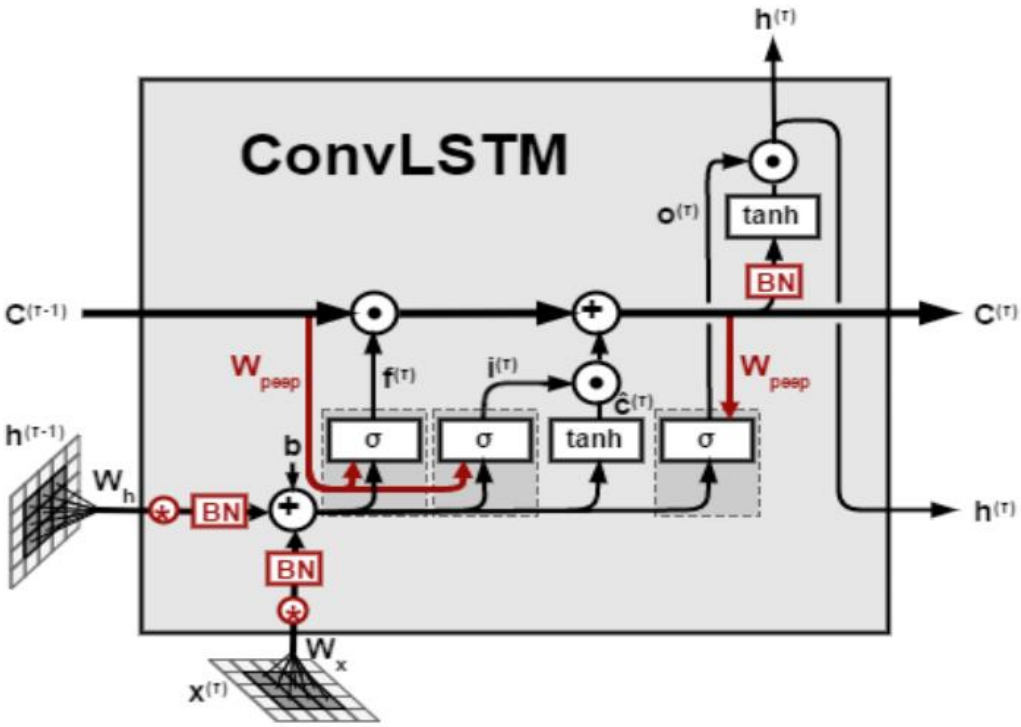

Figure 4.10 Olulana et al LSTM architecture [71]

In [72] (Polat and Mehr) 2019 proposed a hybrid technique composed from 3D-CNN with SVM for detection of lung cancer nodules from CT scan, first they rescale the images from 512x512x512 to 227x227x227 and the features have been extracted by the convolutional layers which ends by 2 fully connected layers that connect all the neurons, a softmax classifier is utilized to categorize CT scan pictures into cancer and non-cancer classes in a straight 3D-CNN architecture as a typical CNN, in addition, the hybrid 3D-CNN used a RBF-based SVM classifier as a classification layer. As a result, SVM can map data to a high-dimensional feature space, which is called separable data, using the RBF kernel., this method provided 91.81% for accuracy, 88.53 and 94.23 for sensitivity and specificity, respectively, for detection cancer.

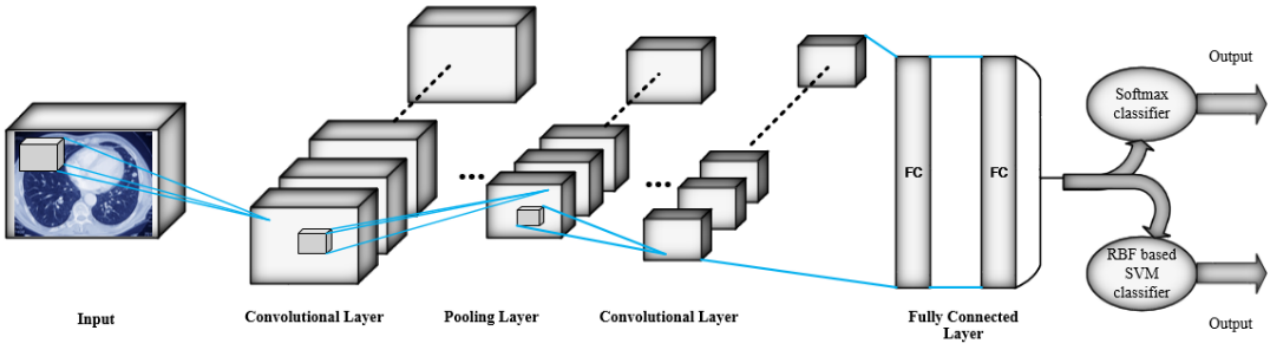

Figure 4.11 Architecture of 3DCNN and two classifiers

In [75] 2020 Sibille et al provided 2D- CNN to classify two datasets one was with Lung Cancer and the second was with lymphoma, where they used for segmentation two experts to do it by using a volume-of-interest tool to classify the lesion into suspicious for cancer or nonsuspicious for cancer, then they used threshold for automatic segmentation, after that thy imported the data to the CNN architecture to classify and localize the disease in both datasets, their methods achieved with the first dataset 88.4% as an accuracy .75.4% sensitivity, 95.8% specificity and 95% as AUC, and for the second dataset the results were (Accuracy: 88.6%, Sensitivity 87.1%, Specificity 99.0%, and AUC 98%)

In [73] proposed another LSTM architecture with CT scans, composed of 4 units each including convolution operations applied separately to each slice and a CONV-LSTM to process the volume slice-by-slice. They implemented a MIL-based network with considering each slice of the CT volume as a sample from a bag, their method achieved an AUC=82%, sensitivity, and specificity of 77% and 74%, respectively

Shankar .K et.al in 2020 [74] used OCS-DL for the classification of lung cancer. Their job was based on using Histogram Equalization (HE) as a pre-processing to enhance the image quality then using two techniques to extract features which were GLCM that provides 10 features (Autocorrelation, Contrast, Correlation, Dissimilarity, Cluster Prominence, Cluster Shade Entropy, Energy, Homogeneity, and Maximum Probability) and GLRLM that provided 5 features (Gray-Level Nonuniformity (GLN), Run Length Nonuniformity (RLN), Run Percentage (RP), Short Run Emphasis (SRE), and Long Run Emphasis (LRE)) then they used the OCS algorithm as optimal features selection to choose the significant features which was the input for the classifier DNN to classify the images figure 4.9 shows their approach . This work achieved accuracy, sensitivity, and specificity were 95.22%, 86.45 %, and 100%, respectively.

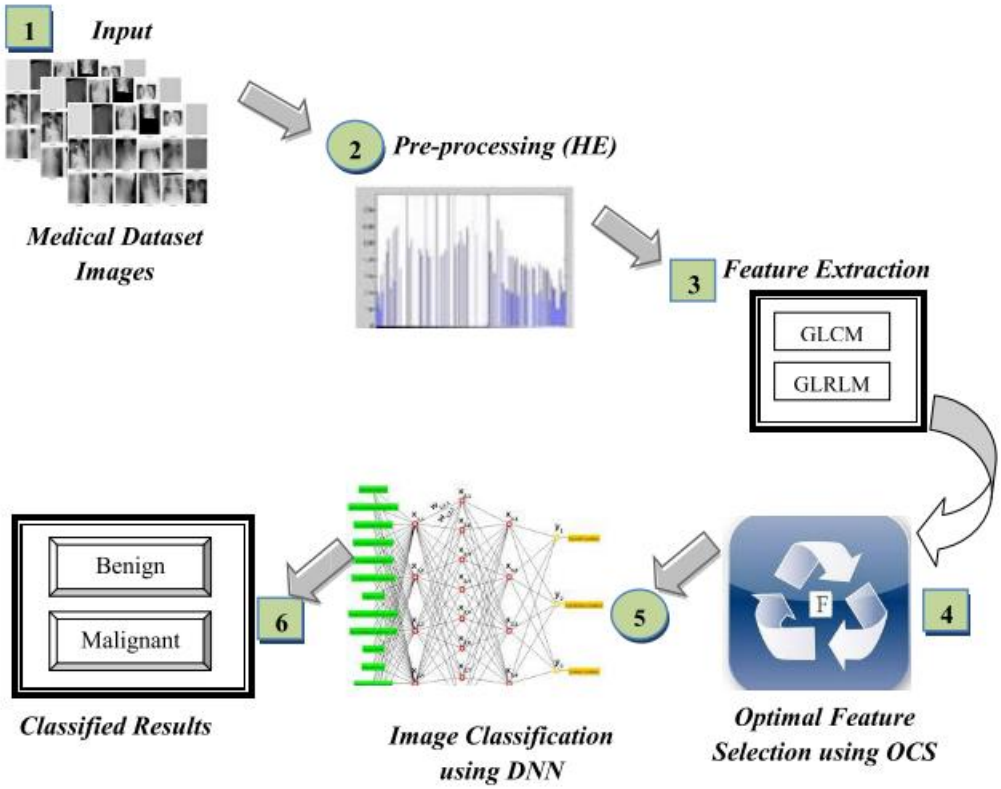

Figure 4.12 Shankar .K architecture [74]

Chapter V

Descoisin and Conclousion

5. Chapter 5: Discussion and Conclusion

5.1 Discussion

The aim of this study was lighting on the most used architecture for segmentation and classification of lung cancer, This study shows that there are many approaches to do segmentation of the lung and classification lung cancer, for segmentation, some papers used U_net for building the binary mask for the lung as Shaziya et.al in 2018 [52], used U_net architecture with 267 CT scans in size 128x128 and applying resize to 32x32, also Kaul et al. 2019 in [60] did the resize for the images from 512x512 to 32x32 and both of those studies contained very low dataset size 267 CT scans and they solved this issue using data augmentation , random zooms and flipping to increase the training images size, data augmentation is a one of methods that researchers using it as it provides more dataset to avoid the overfitting providing an accuracy of 99.32%, sensitivity 97.57%, and specificity 99.8%,, where Men et al. who proposed 2D-CNN used also general data augmentation methods including random scaling (from 0.5 to 1.5), random cropping, and random rotation (-5° to 5°) to avoid overfitting and for compensate the model's lack of training data, they choose high-quality photos from the candidate set to add to the training set for fine-tuning. The architecture of FOCUS_NET and U_NET is similar by down-sampling from one path and up-sampling in the other path which was clear in the U_NET of Hassani, E L, and et.al work and the FOCUS_NET because it was necessary to crop and concatenate corresponding feature maps from the left side with their corresponding feature maps in the other path, in another hand Shaziya et.al did not follow this approach. U_net can be also used for 3d scans which work on the voxel's values instead of pixels where Roth et.al used this technique and they used smooth B-spline deformations to both the picture and label data in training, comparable to. Besides using data augmentation that can artificially increase the training data and encourages convergence to 20 to +20 voxels in each dimension at each iteration to generate convincing deformations during training. The voxels are separated by a 24 voxel grid. they also used random rotations of 20° to +20°, as well as translations of more robust solutions, to reduce overfitting to the training data, their work has been achieved with accuracy reached to 89.4. A different version of U-Net called U_NET++ that used by Zhou. Z et.al [57] where what distinguishes the U_NET++ from U_net is their model started with an encoder sub-network or backbone followed by a decoder sub-network, then the re-designed skipped pathways that connected the two sub-networks and the use of deep supervision is what, as well as the

application of deep supervision, Xiao et al in [58] also used 3DUNet architecture with a combination of Res2Net which contained 23 layers which allowed to capture of very small features. A different way to segment lung cancer is followed by Tan et al.[60] who proposed the LGAN architecture which is based on specific features in the images such as the grayscale features and their Adversarial Network is trained to discriminate segmentation maps from the ground truth and the generator. Another CNN model used for the segmentation that proposed by Xu et al in [61] but instead of using the full images that they have 512x512 they split those images into patches with size 32x32 without overlapping their method achieved with accuracy up to 99.2%, Sensitivity = 98.8%, Specificity= 99.5%, and AUC = 99.91%.

While for classification the lung cancer types have different algorithms used by the researchers, for example, Mhaske. D et al. in 2019 [66] used a combination between LSTM neural network to classify lung cancer and CNN neural network which extracted the features from the 2D images. The CNN architecture contained 22 hidden layers; and before feature extraction, they had to do segmentation using the Otsu threshold, Their LSTM was distinguished by its four gates which are input gate, forget gate, output gate, weights, and bias for the respective gates. Which is different from Gao R et.al [67] approach where they used also LSTM but without combination with other neural network and their distance LSTM had 3 gates, The accuracy of Mhaske. D method was 97% in classification while Gao R et.al method achieved 82.55 for accuracy, another compilation between CNN and LSTM used by Olulana et al 2020 [71] which was their architecture a hybrid algorithm for nodule generation of Lung from CT scans composed from CNN with 3D Convolutional LSTM algorithm and their method achieved 97.2% as accuracy. Another research followed different another architecture which is the Convolution neural network CNN such as Cai et al where they used CNN to classify the patches of the lung images where the patch size was 16x16 and their method has 3 fully connected layers instead of 1 connected layer as a difference from Sibille L et.al where they used also 2D-CNN but with one fully connected layers and their segmentation was manual with two experts to do it by using a volume-of-interest tool their method showed (Accuracy: 88.6%, Sensitivity 87.1%, Specificity 99.0%, and AUC 98%) while in Cai et al approach they achieved accuracy over than 90%. 3DCNN also can be used for the classification as the research of Alakwaa et al [70] and Polat and Mehr [72] were both used 3DCNN but with Alakwaa et al they used 3DU-NET for segmentation to remove all the chest cavity from the images before the classification which contained 2 convolutional layers for feature extraction and one fully connected layer for classification and their method achieved accuracy with 86.6% and AUC

with 83%, while Polat and Mehr method based on rescaling the images and their model end by 2 connected layers which connected with svm classifier that provided 91.81% for accuracy, 88.53 and 94.23 for sensitivity and specificity, respectively. Another method used for classification proposed by Shankar .K et.al in 2020 [74] where they used OCS-DL they followed two techniques to extract features which were GLCM that provides 10 features and GLRLM that provided 5 features which distinguished their method, then they used the OCS algorithm as optimal features selection to use as input for the classifier DNN, This work achieved accuracy, sensitivity, and specificity were 95.22%, 86.45 %, and 100%, respectively.

It is noticeable that many researchers proposed different techniques based on their dataset and the size of the dataset where U_NET was the most used architecture for segmentation as it provides very reliable results based on its way of feature extracting and most of the time it was noticeable that they do some pre-processing before the segmentation such as resize the dataset which helps the CPU that they used to do the training in less time without ruining the RAM. Besides they avoid the lack of the dataset by using the data augmentation that generates new data because most of the time the medical images are not so much to train which creates an overfitting problem, they tried to do a rotation with different angles on both sides, flipping and zooming, and the second most used was CNN which did not provide such good results as U_NET.

On the other hand, the Classification of lung cancer was another review we did in this article where the researchers followed mostly the CNN and secondly the LSTM where some of them made a combination between the two algorithms as the CNN is a powerful architecture for feature extraction from the images which usually either resized into smaller size or they cropped patches from the original images with care to avoid the overlapping between the patches, then fed them to the CNN for the feature extraction which ended by a classifier such as fully connected layer from 2 or 3 layers or with using another architecture to classify such as LSTM, SVM, or K_Mean and it was obvious that by using the combination they able to have better results

5.2 Conclusion

Lung cancer mortality is mostly determined by the early detection and inspection of pulmonary nodules, which must be exact and reliable. This paper provided a brief overview of recently suggested CAD systems that use deep learning to extract features, detect cancer, and classify them as benign or malignant. This research offered a thorough examination of the most recently deep learning models for CT screening detection and categorization. We gave information about 22 articles between segmentation and classification that used several architectures and examined the most up-to-date models such as U_NET, CNN, and LSTM which function for both 2D and 3D datasets. Our research focused on 3 search engines IEEE, GOOGLE SCHOLAR, and PUBMED. We found after comparing the articles and their results that recently many researchers starting to use a combination of two types of the neural network provided better results besides the neural network that has more fully connected layers, this research could be a helpful reference for further studies related the lung scans analyses, as we provided fulfilling information about most used architectures in this field as the approaches they used, the difficulties that found, the ways that built the neural network, pre_proceesing steps, and the ways that show the results. However, there is still a lot of research being done to enhance, speed up, and generalize the CAD system, as existing approaches have flaws that must be addressed through research like when the researchers combine between two architecture which needs more hardware recorses. As a result, a thorough understanding of those models, their benefits, and recent studies in the field of lung cancer detection and classification will aid in the development of CAD systems that will assist radiologists in diagnosing severe diseases like lung cancer, as well as in other areas of medical imaging.

Chapter VI

References

1. Tu J, Inthavong K, Ahmadi G. The Human Respiratory System. Springer, Dordr. 2013;19–44.

2. Terry Des Jardins. The Anatomy and Physiology of the Respiratory System Sagittal Section of Upper Airway ch1. Thomson Delmar Learn. 2008;1–62.

3. Khong TY. The respiratory system. Keeling's Fetal Neonatal Pathol. 2015;531–59.

4. Sohn HY, Kim SK, Kim KH. Anatomy of the Respiratory System. Tuberc. Respir. Dis. (Seoul). 1985.

5. Tomashefski JF, Farver CF. Anatomy and Histology of the Lung. Dail and Hammar's Pulmonary Pathology. 2008;20–48.

6. Parson SH. Clinically Oriented Anatomy, 6th edn. J Anat. 2009;215:474–474.

7. Anatomy GP, Anatomy A. Anatomy of the Lung. Underst Pulm Pathol Appl Pathol Find Ther Decis Mak. 2017;5–19.

8. Ugalde P, Camargo J de J, Deslauriers J. Lobes, Fissures, and Bronchopulmonary Segments. Thorac Surg Clin. 2007;17:587–99.

9. Stanfield CL. Principles of Human Physiology. 5th editio. Med. J. Aust. University of South Alabama; 2013.

10. Sung H, Ferlay J, Siegel RL, Laversanne M, Soerjomataram I, Jemal A, et al. Global Cancer Statistics 2020: GLOBOCAN Estimates of Incidence and Mortality Worldwide for 36 Cancers in 185 Countries. CA Cancer J Clin. 2021;71:209–49.

11. Mustafa M, Azizi AJ, IIIzam E, Nazirah A, Sharifa S, Abbas S. Lung Cancer: Risk Factors, Management, And Prognosis. IOSR J Dent Med Sci. 2016;15:94–101.

12. Cooper WA, Lam DCL, O'Toole SA, Minna JD. Molecular biology of lung cancer. J Thorac Dis. 2013;5.

13. Jakopovic M, Thomas A, Balasubramaniam S, Schrump D, Giaccone G, Bates SE. Targeting the epigenome in lung cancer: Expanding approaches to epigenetic therapy. Front Oncol. 2013;3 OCT:1–12.

14. Mulvihill MS, Kratz JR, Pham P, Jablons DM, He B. The role of stem cells in airway repair: Implications for the origins of lung cancer. Chin J Cancer. 2013;32:71–4.

15. Bueno R, Sugarbaker D, Colson Y, Jaklitsch M, Krasna M, Mentzer S. adult chest surgery. second edi. 2015.

16. Kreisman H, Wolkove N, Quoix E. Small cell lung cancer presenting as a solitary pulmonary nodule. Chest. 1992;101:225–31.

17. Travis WD, Brambilla E, Müller-Hermelink HK, Harris CC eds. Pathology & Genetics of Tumours of the Lung, Pleura, Thymus and Heart. IARC/Press. 2004;344.

18. Khuder SA. Effect of cigarette smoking on major histological types of lung cancer: A meta-analysis. Lung Cancer. 2001;31:139–48.

19. Park CM, Goo JM, Lee HJ, Lee CH, Chung DH, Chun EJ, et al. Focal interstitial fibrosis manifesting as nodular ground-glass opacity: Thin-section CT findings. Eur Radiol. 2007;17:2325–31.

20. Travis WD. Pathology of Lung Cancer. Clin Chest Med [Internet]. Elsevier Inc; 2011;32:669–92.

21. Pelosi G, Barbareschi M, Cavazza A, Graziano P, Rossi G, Papotti M. Large cell carcinoma of the lung: A tumor in search of an author. A clinically oriented critical reappraisal. Lung Cancer [Internet]. Elsevier Ireland Ltd; 2015;87:226–31.

22. Travis WD, Linnoila RI, Tsokos MG, Hitchcock CL, Cutler GB, Nieman L, et al. Neuroendocrine Tumors of the Lung With Proposed Criteria for Large-Cell Neuroendocrine Carcinoma. Am. J. Surg. Pathol. 1991. p. 529–53.

23. Kocher F, Hilbe W, Seeber A, Pircher A, Schmid T, Greil R, et al. Longitudinal analysis of 2293 NSCLC patients: A comprehensive study from the TYROL registry. Lung Cancer [Internet]. Elsevier Ireland Ltd; 2015;87:193–200.

24. Saettele TM, Ost DE. Multimodality systematic approach to mediastinal lymph node staging in non-small cell lung cancer. Respirology. 2014;19:800–8.

25. Fischer BM, Mortensen J, Hansen H, Vilmann P, Larsen SS, Loft A, et al. Multimodality approach to mediastinal staging in non-small cell lung cancer. Faults and benefits of PET-CT: A randomised trial. Thorax. 2011;66:294–300.

26. Mehta AC, Marty JJ, Lee FYW. Sputum cytology. Clin Chest Med. 1993;14:69–85.

27. Medenica M, Medenica M, Cosovic D. Pleural Effusions in Lung Cancer: Detection and

Treatment. Lung Cancer - Strateg Diagnosis Treat. 2018;

28. Call S, Sánchez D, Rami-Porta R. Diagnosis and treatment of malignant pleural effusion. Malig Effusions Pleuritis, Ascites, Pericardites. 2012;23–55.

29. Bartlett EC, Devaraj A. Imaging Techniques in Lung Cancer. Ref Modul Biomed Sci. 2011;7:338–46.

30. Schaefer-Prokop C, Prokop M. New imaging techniques in the treatment guidelines for lung cancer. Eur Respir Journal, Suppl. 2002;19:71–83.

31. Nitrosi A, Borasi G, Nicoli F, Modigliani G, Botti A, Bertolini M, et al. A filmless radiology department in a full digital regional hospital: Quantitative evaluation of the increased quality and efficiency. J Digit Imaging. 2007;20:140–8.

32. MacMahon H, Li F, Engelmann R, Roberts R, Armato S. Dual energy subtraction and temporal subtraction chest radiography. J Thorac Imaging. 2008;23:77–85.

33. Kalra MK, Maher MM, Toth TL, D'Souza R, Saini S. Multidetector computed tomography technology: Current status and emerging developments. J Comput Assist Tomogr. 2004;28:2–6.

34. Prokop M. General principles of MDCT. Eur J Radiol. 2003;45:S4.

35. Finkelstein SE, Summers RM, Nguyen DM, Stewart IV JH, Tretler JA, Schrump DS. Virtual bronchoscopy for evaluation of malignant tumors of the thorax. J Thorac Cardiovasc Surg. 2002;123:967–72.

36. Schmidt GP, Reiser MF, Baur-Melnyk A. Whole-body MRI for the staging and follow-up of patients with metastasis. Eur J Radiol. 2009;70:393–400.

37. Pauwels EKJ, Mccready VR, Stoot JHMB, Deurzen DFP Van. <The mechanism of accumulation of tumour-localising rp.pdf>. 1998;25.

38. Burger C, Goerres G, Schoenes S, Buck A, Lonn A, Von Schulthess G. PET attenuation coefficients from CT images: Experimental evaluation of the transformation of CT into PET 511-keV attenuation coefficients. Eur J Nucl Med. 2002;29:922–7.

39. Bar-Shalom R, Yefremov N, Guralnik L, Gaitini D, Frenkel A, Kuten A, et al. Clinical performance of PET/CT in evaluation of cancer: Additional value for diagnostic imaging and patient management. J Nucl Med. 2003;44:1200–9.

40. Kota VM, Manoj Kumar V, Bharatiraja C. Deep Learning - A Review. IOP Conf Ser Mater Sci Eng. 2020;912.

41. Lecun Y, Bengio Y, Hinton G. Deep learning. Nature. 2015;521:436–44.

42. Hiriyannaiah S, Srinivas AMD, Shetty GK, G.M. S, Srinivasa KG. A computationally intelligent agent for detecting fake news using generative adversarial networks [Internet]. Hybrid Comput. Intell. INC; 2020.

43. Bengio Y, Simard P, Frasconi P. Learning Long-Term Dependencies with Gradient Descent is Difficult. IEEE Trans Neural Networks. 1994;5:157–66.

44. Ruiz L, Vargas R. Deep Learning: Previous and Present Applications. J Aware. 2017;2:11,13.

45. Mosavi A, Vaezipour A. Reactive Search Optimization; Application to Multiobjective Optimization Problems. Appl Math. 2012;03:1572–82.

46. Lee TS, Mumford D. Hierarchical Bayesian inference in the visual cortex. J Opt Soc Am A. 2003;20:1434.

47. Letters IP, Kc L. Deep Neural Networks – A Brief History Krzysztof. Inf Process Lett. 2018;30:19–20.

48. Delrue L, Gosselin R, Ilsen B, Van Landeghem A, de Mey J, Duyck P. Difficulties in the Interpretation of Chest Radiography. 2011;27–49.

49. Mittal A, Hooda R, Sofat S. Lung field segmentation in chest radiographs: A historical review, current status, and expectations from deep learning. IET Image Process. 2017;11:937–52.

50. Bala GM, Aroquiaraj IL. Lung Cancer Image Segmentation And Classification Using Soft Computing Techniques. 2016;6:120–6.

51. lung cancer segmentation using neural network [Internet]. Pubmed. [cited 2021 Sep 8]. Available from: https://pubmed.ncbi.nlm.nih.gov/?term=lung+cancer+segmentation+using+neural+network

52. Almotairi S, Kareem G, Aouf M, Almutairi B, Salem MAM. Liver tumor segmentation in CT scans using modified segnet. Sensors (Switzerland). 2020;20.

53. El A, Hassani EL, Majda A, Ait B. ScienceDirect ScienceDirect ScienceDirect Lung CT

CT Image Image Segmentation Segmentation Using Using Deep Deep Neural Neural Networks Networks. Procedia Comput Sci [Internet]. Elsevier B.V.; 2018;127:109–13.

54. Men K, Geng H, Biswas T, Liao Z, Xiao Y. Automated Quality Assurance of OAR Contouring for Lung Cancer Based on Segmentation With Deep Active Learning. 2020;10:1–7.

55. Hu Q, Luís LF, Holanda GB, Alves SSA, Francisco FH, Han T, et al. An effective approach for CT lung segmentation using mask region-based convolutional neural networks. Artif Intell Med. 2020;103.

56. Roth HR, Shen C, Oda H, Oda M, Hayashi Y, Misawa K, et al. Deep learning and its application to medical image segmentation. 2018;36:63–71

57. Zhou Z, Rahman Siddiquee MM, Tajbakhsh N, Liang J. Unet++: A nested u-net architecture for medical image segmentation [Internet]. Lect. Notes Comput. Sci. (including Subser. Lect. Notes Artif. Intell. Lect. Notes Bioinformatics). Springer International Publishing; 2018.

58. Xiao Z, Liu B, Geng L, Zhang F, Liu Y. Segmentation of lung nodules using improved 3D-UNet neural network. Symmetry (Basel). 2020;12:1–15.

59. Kaul C, Manandhar S, Pears N. Focusnet: An attention-based fully convolutional network for medical image segmentation. arXiv. IEEE; 2019;455–8.

60. Tan J, Jing L, Huo Y, Li L, Akin O, Tian Y. LGAN: Lung segmentation in CT scans using generative adversarial network. Comput Med Imaging Graph [Internet]. Elsevier Ltd; 2021;87:101817.

61. Xu M, Qi S, Yue Y, Teng Y, Xu L, Yao Y, et al. Segmentation of lung parenchyma in CT images using CNN trained with the clustering algorithm generated dataset 08 Information and Computing Sciences 0801 Artificial Intelligence and Image Processing Robert Koprowski. Biomed Eng Online [Internet]. BioMed Central; 2019;18:1–21.

62. Liu C, Zhao R, Pang M. A fully automatic segmentation algorithm for CT lung images based on random forest. Med Phys. 2020;47:518–29.

63. Baek S, He Y, Allen BG, Buatti JM, Smith BJ, Tong L, et al. Deep segmentation networks predict survival of non-small cell lung cancer. Sci Rep. 2019;9:1–10.

64. lung cancer classification using neural network [Internet]. [cited 2021 Sep 8]. Available from:
https://pubmed.ncbi.nlm.nih.gov/?term=lung+cancer+classification+using+neural+network

65. Song J, Chi Z, Liu J, Fu H. Bark classification by combining grayscale and binary texture features. 2004 Int Symp Intell Multimedia, Video Speech Process ISIMP 2004. 2004;450–3.

66. Mhaske D, Rajeswari K, Tekade R. Deep learning algorithm for classification and prediction of lung cancer using CT scan images. Proc - 2019 5th Int Conf Comput Commun Control Autom ICCUBEA 2019. 2019;

67. Gao R, Huo Y, Bao S, Tang Y, Antic SL, Epstein ES, et al. Distanced LSTM: Time-Distanced Gates in Long Short-Term Memory Models for Lung Cancer Detection. Lect Notes Comput Sci (including Subser Lect Notes Artif Intell Lect Notes Bioinformatics). 2019;11861 LNCS:310–8.

68. Li Q, Cai W, Wang X, Zhou Y, Feng DD, Chen M. Medical image classification with convolutional neural network. 2014 13th Int Conf Control Autom Robot Vision, ICARCV 2014. 2014;2014:844–8.

69. Lakshmanaprabu SK, Mohanty SN, Shankar K, Arunkumar N, Ramirez G. Optimal deep learning model for classification of lung cancer on CT images. Futur Gener Comput Syst [Internet]. Elsevier B.V.; 2019;92:374–82.

70. Alakwaa W, Nassef M, Badr A. Lung cancer detection and classification with 3D convolutional neural network (3D-CNN). Int J Biol Biomed Eng. 2017;11:66–73.

71. Olulana K, Owolawi P, Tu C, Abe B. Nodule Generation of Lung CT Images Using a 3D Convolutional LSTM Network. Lect Notes Comput Sci (including Subser Lect Notes Artif Intell Lect Notes Bioinformatics). 2020;12510 LNCS:753–60.

72. Polat H, Mehr HD. Classification of pulmonary CT images by using hybrid 3D-deep convolutional neural network architecture. Appl Sci. 2019;9.

73. Braman N, Beymer D, Dehghan E. Disease Detection in Weakly Annotated Volumetric Medical Images using a Convolutional LSTM Network. arXiv [Internet]. 2018

74. Raj RJS, Shobana SJ, Pustokhina IV, Pustokhin DA, Gupta D, Shankar K. Optimal feature selection-based medical image classification using deep learning model in internet of medical things. IEEE Access. 2020;8:58006–17.

75. Chaunzwa TL, Hosny A, Xu Y, Shafer A, Diao N, Lanuti M, et al. Deep learning classification of lung cancer histology using CT images. Sci Rep [Internet]. Nature Publishing Group UK; 2021;1–12.